

# A Family of Highly Ordered Mesoporous Polymer Resin and Carbon Structures from Organic–Organic Self-Assembly

Yan Meng,<sup>†</sup> Dong Gu,<sup>†</sup> Fuqiang Zhang,<sup>†</sup> Yifeng Shi,<sup>†</sup> Liang Cheng,<sup>†</sup> Dan Feng,<sup>†</sup> Zhangxiong Wu,<sup>†</sup> Zhenxia Chen,<sup>†</sup> Ying Wan,<sup>†,‡</sup> Andreas Stein,<sup>§</sup> and Dongyuan Zhao<sup>\*,†,||</sup>

Department of Chemistry, Shanghai Key Lab of Molecular Catalysis and Innovative Materials, and Key Lab of Molecular Engineering of Polymers and Engineering Center of Coating of Chinese Ministry of Education, Fudan University, Shanghai 200433, People's Republic of China, Department of Chemistry, Shanghai Normal University, Shanghai 200234, People's Republic of China, and Department of Chemistry, University of Minnesota, Minneapolis, Minnesota 55455

Received April 21, 2006. Revised Manuscript Received July 2, 2006

The syntheses of a family of highly ordered mesoporous polymers and carbon frameworks from organic–organic assembly of triblock copolymers with soluble, low-molecular-weight phenolic resin precursors (resols) by an evaporation induced self-assembly strategy have been reported in detail. The family members include two-dimensional hexagonal (space group,  $p6m$ ), three-dimensional bicontinuous ( $la\bar{3}d$ ), body-centered cubic ( $Im\bar{3}m$ ), and lamellar mesostructures, which are controlled by simply adjusting the ratio of phenol/template or poly(ethylene oxide)/poly(propylene oxide) in the templates. A five-step mechanism from organic–organic assembly has been demonstrated. Cubic FDU-14 with a gyroidal mesostructure of polymer resin or carbon has been synthesized for the first time by using the copolymer Pluronic P123 as a template in a relatively narrow range. Upon calcination at 350 °C, the templates should be removed to obtain mesoporous polymers, and further heating at above a critical temperature of 600 °C transforms the mesoporous polymers to the homologous carbon frameworks. The mesoporous polymer resin and carbon product materials exhibit ordered structures, high surface areas, (670–1490 m<sup>2</sup>/g), large pore volumes (0.65–0.85 cm<sup>3</sup>/g), and uniform, large pore sizes (7.0–3.9 nm), as well as very thick pore walls (6–8 nm). The carbon open frameworks with covalently bonded constructions and thick pore walls exhibit high thermal stability (>1400 °C). Our results show that the feed gas used during the calcination has a great influence on the porosity of the products. The presence of a small amount of oxygen facilitates the large pore sizes and high surface areas of mesoporous materials with different mesostructures. An extraction method employing sulfuric acid can also decompose the template from hexagonal mesostructured polymers with little framework shrinkage. Preliminary studies of the mechanical and electrochemical properties of mesoporous carbon molecular sieves are also presented.

## Introduction

Supramolecular self-assembly provides routes to a range of materials with diverse multicomponent structures of atoms, ions, and/or molecules, held together by weak noncovalent interactions such as hydrogen bonds, van der Waals forces,  $\pi$ – $\pi$  interactions, and/or electrostatic effects.<sup>1</sup> The weak interactions can drive inorganic–organic assembly<sup>2–4</sup> and organic–organic assembly<sup>5,6</sup> to form inorganic and organic frameworks, respectively. The former has generated an

enormous variety of ordered inorganic mesostructures that have sparked great contributions owing to their large surface areas, uniform pore sizes, and numerous potential applications in separation, catalysis, adsorption, bioreactors, dielectrics, and sensors.<sup>7–11</sup> For example, many periodic mesoporous silicate structures, such as two-dimensional (2-D) hexagonal (space group,  $p6m$ ),<sup>2,4</sup> three-dimensional (3-D) cubic ( $la\bar{3}d$ ,  $Im\bar{3}m$ ,  $Pm\bar{3}n$ , and  $Fm\bar{3}m$ ),<sup>3,12,13</sup> 3-D hexagonal ( $P6_3/mmc$ ),<sup>13</sup> and tetragonal ( $P4/mmm$  and  $P4_2/mnm$ )<sup>14</sup>

\* To whom correspondence should be addressed. E-mail: dyzhao@fudan.edu.cn. Tel.: 86-21-6564-2036. Fax: 86-21-6564-1740.

<sup>†</sup> Department of Chemistry, Shanghai Key Lab of Molecular Catalysis and Innovative Materials, Fudan University.

<sup>‡</sup> Shanghai Normal University.

<sup>§</sup> University of Minnesota.

<sup>||</sup> Key Lab of Molecular Engineering of Polymers and Engineering Center of Coating of Chinese Ministry of Education, Fudan University.

(1) Lehn, J. M. *Angew. Chem., Int. Ed. Engl.* **1990**, *29*, 1304.

(2) Beck, J. S.; et al. *J. Am. Chem. Soc.* **1992**, *114*, 10834.

(3) Huo, Q.; Margolese, D. I.; Ciesla, U.; Feng, P.; Gier, T. E.; Sieger, P.; Leon, R.; Petroff, P. M.; Schuth, F.; Stucky, G. D. *Nature* **1994**, *368*, 317.

(4) Zhao, D. Y.; Feng, J. L.; Huo, Q. S.; Melosh, N.; Fredrickson, G. H.; Chmelka, B. F.; Stucky, G. D. *Science* **1998**, *279*, 548.

(5) Klok, H. A.; Lecommandoux, S. *Adv. Mater.* **2001**, *13*, 1217.

(6) Zeng, F. W.; Zimmerman, S. C. *Chem. Rev.* **1997**, *97*, 681.

(7) Ying, J. Y.; Mehnert, C. P.; Wong, M. S. *Angew. Chem., Int. Ed.* **1999**, *38*, 56.

(8) Baskaran, S.; Liu, J.; Domansky, K.; Kohler, N.; Li, X. H.; Coyle, C.; Fryxell, G. E.; Thevuthasan, S.; Williford, R. E. *Adv. Mater.* **2000**, *12*, 291.

(9) Zhao, J. W.; Gao, F.; Fu, Y. L.; Jin, W.; Yang, P. Y.; Zhao, D. Y. *Chem. Commun.* **2002**, 752.

(10) He, X.; Antonelli, D. *Angew. Chem., Int. Ed.* **2001**, *41*, 214.

(11) Yamada, T.; Zhou, H. S.; Uchida, H.; Tomita, M.; Ueno, Y.; Ichino, T.; Honma, I.; Asai, K.; Katsube, T. *Adv. Mater.* **2002**, *14*, 812.

(12) Liu, X. Y.; Tian, B. Z.; Yu, C. Z.; Gao, F.; Xie, S. H.; Tu, B.; Che, R. C.; Peng, L. M.; Zhao, D. Y. *Angew. Chem., Int. Ed.* **2002**, *41*, 3876.

(13) Zhao, D. Y.; Huo, Q. S.; Feng, J. L.; Chmelka, B. F.; Stucky, G. D. *J. Am. Chem. Soc.* **1998**, *120*, 6024.

(14) (a) Zhao, D. Y.; et al. *J. Am. Chem. Soc.* **2005**, *127*, 6780. (b) Garcia-Bennett, A. E.; Kupferschmidt, N.; Sakamoto, Y.; Che, S.; Terasaki, O. *Angew. Chem., Int. Ed.* **2005**, *44*, 5317.

mesostructures, have been synthesized by using amphiphilic surfactants or/and block copolymer self-assembly. As a result of weak interaction as well as different thermal and chemical stabilities between the inorganic frameworks and the organic templates, ordered mesoporous silicates with strong covalently bonded infinite inorganic frameworks are easily obtained after template removal by either calcination or solvent extraction.<sup>13,15</sup> The inorganic-organic self-assembly has been successfully extended to synthesize ordered mesoporous metal oxides,<sup>3,16-19</sup> metal sulfides,<sup>20-22</sup> and even metals.<sup>23,24</sup> However, the preparation of mesoporous carbon materials with ordered open pore structures is extremely difficult in solution and remains challenging because of the high formation energy of C-C bonds. Significant research activity has been undertaken to develop mesoporous carbons due to their enormous potential for many high-tech applications such as hydrogen storage, catalysis, adsorption, separations, electrochemical double capacitors, and even semiconductor and space technologies.<sup>25-28</sup> A frequently used approach to fabricate ordered mesoporous carbon materials is a nanocasting procedure which utilizes mesoporous silicate as a hard template.<sup>29</sup> These kinds of mesoporous carbons are constructed as ordered nanowire, nanorod, or nanotube arrays, replicating the ordered structures of mesoporous silicates. Mesoporous carbon replicas can be prepared through several steps: filling of the carbon sources into the mesoporous silica channels, carbonization, and etching of the hard silicate templates by use of HF or NaOH solution. It is an obviously elaborate, high-cost, and thus industrially unfeasible method. Therefore, a soft supramolecular self-assembly approach toward ordered mesoporous carbons with open frameworks is desirable.

Nanoporous organic materials are quite different from their inorganic counterparts as a result of the intrinsic character of organic molecules. In general, these materials can be fabricated through several routes including controlled foaming,<sup>30,31</sup> ion track etching,<sup>32</sup> molecular imprinting,<sup>33,34</sup> phase

separation,<sup>35,36</sup> and a hard templating approach by employing colloidal particles<sup>37,38</sup> or porous inorganic materials.<sup>39</sup> The latter two methods have been widely exploited to prepare ordered polymer mesostructures. However, ordered mesoporous polymer channels with large surface area and porosity have not been obtained yet, perhaps because of the lack of covalently bonded frameworks. Gin and co-workers<sup>40</sup> prepared periodic organic mesostructures by a procedure of cross-linking lyotropic liquid crystals in an aqueous solution. Unfortunately, the polymerization of liquid crystals only occurs at the nearest neighbor headgroups of surfactant molecules around the water core, and the pore channels are occupied with water molecules, resulting in no porosity.

Organic-organic self-assembly has been applied to synthesizing organic nanostructures and carbon materials via carbonization. Mesostructured organic materials have been made by polymerizing an organic monomer in either the hydrophobic or the aqueous phase of a surfactant/water or solvent/organic monomer ternary mixture,<sup>33,41-43</sup> such as a mesoporous polyacrylonitrile structure from self-assembly of the triblock copolymer poly(propylene oxide)-*b*-poly(ethylene oxide)-*b*-poly(propylene oxide) (PO<sub>19</sub>-EO<sub>33</sub>-PO<sub>19</sub>) in aqueous solution, and nanoporous carbon prepared by assembling cetyltrimethylammonium bromide (CTAB) with resorcinol/formaldehyde in solution. Their structures were, however, disordered. The main reason may be the extremely weak interaction between organic polymer frameworks and amphiphilic surfactants. It results in the reduction of miscibility between organic frameworks and surfactants after polymerization and consequent macroscopic phase separation. Hillmyer and co-workers<sup>35,44</sup> synthesized polymer nanostructure by using low-molecular-weight thermosetting epoxy as an organic precursor and diblock copolymer poly(ethylene oxide)-*b*-poly(ethylene glycol) (PEO-PEG) as a template. The interaction between the epoxy resin precursor and the template is stronger than that inside the resin precursor itself. Hence, highly ordered polymer nanostructures could be obtained via organic-organic self-assembly, and subsequent cross-linkage of the epoxy matrix did not destroy the nanostructures. Unfortunately, template removal and evidence for porosity in the products were not reported.

- (15) (a) Tian, B. Z.; Liu, X. Y.; Yu, C. Z.; Gao, F.; Luo, Q.; Xie, S. H.; Tu, B.; Zhao, D. Y. *Chem. Commun.* **2002**, 1186. (b) Yang, C. M.; Zibrowius, B.; Schmidt, W.; Schuth, F. *Chem. Mater.* **2003**, *15*, 3739.
- (16) Antonelli, D. M.; Ying, J. Y. *Angew. Chem., Int. Ed.* **1996**, *35*, 26.
- (17) Yang, P. D.; Zhao, D. Y.; Margolese, D. I.; Chmelka, B. F.; Stucky, G. D. *Nature* **1998**, *396*, 152.
- (18) Tian, B. Z.; Liu, X. Y.; Tu, B.; Yu, C. Z.; Fan, J.; Wang, L. M.; Xie, S. H.; Stucky, G. D.; Zhao, D. Y. *Nat. Mater.* **2003**, *2*, 1593.
- (19) Schuth, F. *Chem. Mater.* **2001**, *13*, 3184.
- (20) Braun, P. V.; Osenar, P.; Tøhver, V.; Kennedy, S. B.; Stupp, S. I. *J. Am. Chem. Soc.* **1999**, *121*, 7302.
- (21) Froba, M.; Oberender, N. *Chem. Commun.* **1997**, 1729.
- (22) Braun, P. V.; Osenar, P.; Stupp, S. I. *Nature* **1996**, *380*, 325.
- (23) Attard, G. S.; Goltner, C. G.; Corker, J. M.; Henke, S.; Templer, R. H. *Angew. Chem., Int. Ed. Engl.* **1997**, *36*, 315.
- (24) Attard, G. S.; Bartlett, P. N.; Coleman, N. R. B.; Elliott, J. M.; Owen, J. R.; Wang, J. H. *Science* **1997**, *278*, 838.
- (25) Lee, J.; Yoon, S.; Hyeon, T.; Oh, S. M.; Kim, K. B. *Chem. Commun.* **1999**, 2177.
- (26) Planeix, J. M.; Coustel, N.; Coq, B.; Brotons, V.; Kumbhar, P. S.; Dutartre, R.; Geneste, P.; Bernier, P.; Ajayan, P. M. *J. Am. Chem. Soc.* **1994**, *116*, 7935.
- (27) Dillon, A. C.; Jones, K. M.; Bekkedahl, T. A.; Kiang, C. H.; Bethune, D. S.; Heben, M. J. *Nature* **1997**, *386*, 377.
- (28) Yu, J. S.; Kang, S.; Yoon, S. B.; Chai, G. J. *Am. Chem. Soc.* **2002**, *124*, 9382.
- (29) Ryou, R.; Joo, S. H.; Kruk, M.; Jaroniec, M. *Adv. Mater.* **2001**, *13*, 677.
- (30) Krause, B.; Sijbesma, H. J. P.; Munuklu, P.; van der Vegt, N. F. A.; Wessling, M. *Macromolecules* **2001**, *34*, 8792.

- (31) Krause, B.; Koops, G. H.; van der Vegt, N. F. A.; Wessling, M.; Wubbenhorst, M.; van Turnhout, J. *Adv. Mater.* **2002**, *14*, 1041.
- (32) Martin, C. R. *Chem. Mater.* **1996**, *8*, 1739.
- (33) Hentze, H. P.; Antonietti, M. *Curr. Opin. Solid State Mater. Sci.* **2001**, *5*, 343.
- (34) Wulff, G. *Chem. Rev.* **2002**, *102*, 1.
- (35) (a) Zalusky, A. S.; Olayo-Valles, R.; Wolf, J. H.; Hillmyer, M. A. *J. Am. Chem. Soc.* **2002**, *124*, 12761. (b) Rzaev, J.; Hillmyer, M. A. *J. Am. Chem. Soc.* **2005**, *127*, 13373.
- (36) Jenekhe, S. A.; Chen, X. L. *Science* **1999**, *283*, 372.
- (37) Jiang, P.; Hwang, K. S.; Mittleman, D. M.; Bertone, J. F.; Colvin, V. L. *J. Am. Chem. Soc.* **1999**, *121*, 11630.
- (38) Johnson, S. A.; Ollivier, P. J.; Mallouk, T. E. *Science* **1999**, *283*, 963.
- (39) Kim, J. Y.; Yoon, S. B.; Kooli, F.; Yu, J. S. *J. Mater. Chem.* **2001**, *11*, 2912.
- (40) (a) Smith, R. C.; Fischer, W. M.; Gin, D. L. *J. Am. Chem. Soc.* **1997**, *119*, 4092. (b) Gin, D. L.; Gu, W. Q.; Pindzola, B. A.; Zhou, W. J. *Acc. Chem. Res.* **2001**, *34*, 973.
- (41) Zhu, X. X.; Banana, K.; Yen, R. *Macromolecules* **1997**, *30*, 3031.
- (42) Lee, K. T.; Oh, S. M. *Chem. Commun.* **2002**, 2722.
- (43) Jang, J.; Bae, J. *Chem. Commun.* **2005**, 1200.
- (44) Hillmyer, M. A.; Lipic, P. M.; Hajduk, D. A.; Almdal, K.; Bates, F. S. *J. Am. Chem. Soc.* **1997**, *119*, 2749.

More recently, Dai and co-workers<sup>45</sup> successfully prepared ordered mesoporous carbon films with open pore structures by employing resorcinol and formaldehyde as carbon sources and the diblock copolymer poly(styrene)-*b*-poly(4-vinylpyridine) (PS-*b*-P4VP) as a template. Similar results were reported by Tanaka et al.,<sup>46</sup> in which the same carbon precursor and Pluronic F127 (EO<sub>106</sub>-PO<sub>70</sub>-EO<sub>106</sub>) were used for organic-organic self-assembly. Remarkably, triethyl orthoacetate (EOA) was added as a carbon co-precursor, which may decrease the polymerization rate of resorcinol and formaldehyde under strong acid conditions and enhance the interaction between them and the surfactant templates. Kosonen and co-workers used assembly of the novolac phenolic resin and diblock copolymer PS-*b*-P4VP to prepare porous nanostructures under acidic conditions. Unfortunately, the resulting materials are disordered with very low porosity.<sup>47</sup> Consequently, the interactions between both organic precursors and templates and the organic precursors themselves should be considered in an organic-organic assembly for preparing ordered mesoporous polymers and carbons with diversified structures, especially for the common strategies such as hydrothermal treatment<sup>2,4</sup> or the solvent evaporation induced self-assembly (EISA) method.<sup>48,49</sup> One can then expect a proliferation of organic mesostructures similar to that for mesoporous silicates.

We demonstrated a reproducible synthesis of highly ordered mesoporous polymers and carbons from solvent EISA of low-molecular-weight and water-soluble phenolic resins (resols) and low-cost, commercial triblock copolymers PEO-PPO-PEO.<sup>50</sup> The resols are polymerized by phenol and formaldehyde under an alkaline condition and have plenty of hydroxyl groups (-OH), which can strongly interact with copolymer templates via hydrogen bonds.<sup>51</sup> A simple thermopolymerization at low temperatures can transform the soluble resols to cross-linked phenolic resins which possess network structures with benzene rings as three or four cross-linking points.<sup>52</sup> This structural feature is analogous to that of the microporous zeolites which are made of four-connected silicate tetrahedrons and has a covalently bonded infinite framework.

Here we report a systematic study of the synthesis of a family of highly ordered mesoporous polymer resin and carbon structures with high surface areas and uniform pore sizes by the organic-organic assembly of copolymers PEO-PPO-PEO with resols via an EISA strategy. The family

members include 2-D hexagonal (*p6m*), 3-D cubic (*Im $\bar{3}m$* ), 3-D bicontinuous (*Ia $\bar{3}d$* ), and lamellar mesostructures. Attractive 3-D cubic FDU-14 with a gyroidal mesostructure is a new family member which is synthesized by using the EISA method with copolymer P123 as a template. A five-step mechanism from organic-organic assembly is for the first time demonstrated. Simply increasing the ratio of phenol/template and the PEO/PPO segment in triblock copolymer can generate the mesostructure with a high curvature. A mesophase diagram is first reported. Two simple methods to remove the surfactant templates are reported in detail. Heating the as-made organic materials at 350 °C under argon or nitrogen atmosphere results in decomposition of the templates and formation of ordered mesoporous polymers with various mesostructures. Heated at a temperature above 600 °C, ordered polymers transform to homologous carbon frameworks. This temperature is critical to distinguish these two kinds of frameworks. Notably, a small amount of oxygen in the feed gas during the calcination process facilitates the degradation of templates and organic segments and, thus, the formation of large pore sizes and high surface areas (1490 m<sup>2</sup>/g). Besides calcination, a new method of sulfuric acid-aided extraction can remove the template from the hexagonal mesostructured polymers. By comparison with the anti-phase carbons replicated by mesoporous silicates, the framework integrity is maintained in the mesoporous carbons described in our work, benefiting the mechanical stability and the reversible lithium ion capacity of the porous carbon.

## Experimental Section

**Chemicals.** Triblock copolymers Pluronic P123 ( $M_w = 5800$ , EO<sub>20</sub>-PO<sub>70</sub>-EO<sub>20</sub>) and Pluronic F127 ( $M_w = 12\ 600$ , EO<sub>106</sub>-PO<sub>70</sub>-EO<sub>106</sub>) were purchased from Acros Corp. Pluronic F108 ( $M_w = 14\ 600$ , EO<sub>132</sub>-PO<sub>50</sub>-EO<sub>132</sub>) was purchased from BASF Corp. Other chemicals were purchased from Shanghai Chemical Corp. All chemicals were used as received without any further purification. Millipore water was used in all experiments.

**Synthesis of Resol Precursors.** Resol, a low-molecular-weight, soluble phenolic resin, was prepared from phenol and formaldehyde in a base-catalyzed process. In a typical procedure, 0.61 g of phenol was melted at 40–42 °C in a flask and mixed with 0.13 g of 20 wt % sodium hydroxide (NaOH) aqueous solution under stirring. After 10 min, 1.05 g of formalin (37 wt % formaldehyde) was added dropwise below 50 °C. Upon further stirring for 1 h at 70–75 °C, the mixture was cooled to room temperature. The pH was adjusted with 0.6 M HCl solution until it reached a value of ~7.0, and water was removed by vacuum evaporation below 50 °C. The final product was dissolved in ethanol. The molar ratio of phenol/formaldehyde/NaOH was 1:2:0.1. The weight-average molecular weight of resol precursors used in this paper was smaller than 500, which was determined by gel permeation chromatography (GPC).

**Synthesis of FDU-15 Mesoporous Polymers and Carbons with Hexagonal Structure.** FDU-15 samples were synthesized by a solvent EISA method with copolymers F127 or P123 as a template in an ethanol solution. The synthesis compositions were in the range of phenol/formaldehyde/NaOH/F127 (molar ratio) = 1:2:0.1:0.010–0.015 or phenol/formaldehyde/NaOH/P123 = 1:2:0.1:0.007–0.016. In a typical preparation, 1.0 g of F127 was dissolved in 20.0 g of ethanol. Then 5.0 g of resol precursors in ethanol solution containing 0.61 g of phenol and 0.39 g of formaldehyde was added. After stirring for 10 min, a homogeneous solution was obtained. The

(45) Liang, C. D.; Hong, K. L.; Guiochon, G. A.; Mays, J. W.; Dai, S. *Angew. Chem., Int. Ed.* **2004**, *43*, 5785.

(46) Tanaka, S.; Nishiyama, N.; Egashira, Y.; Ueyama, K. *Chem. Commun.* **2005**, 2125.

(47) Kosonen, H.; Valkama, S.; Nykanen, A.; Toivanen, M.; Brinke, G.; Ruokolainen, J.; Ikkala, O. *Adv. Mater.* **2006**, *18*, 201

(48) Brinker, C. J.; Lu, Y. F.; Sellinger, A.; Fan, H. Y. *Adv. Mater.* **1999**, *11*, 579.

(49) Soler-Illia, G.; Crepaldi, E. L.; Grosso, D.; Sanchez, C. *Curr. Opin. Colloid Interface Sci.* **2003**, *8*, 109.

(50) Meng, Y.; Gu, D.; Zhang, F. Q.; Shi, Y. F.; Yang, H. F.; Li, Z.; Yu, C. Z.; Tu, B.; Zhao, D. Y. *Angew. Chem., Int. Ed.* **2005**, *44*, 7053.

(51) (a) Chu, P. P.; Wu, H. D. *Polymer* **2000**, *41*, 101. (b) Kosonen, H.; Ruokolainen, J.; Torckeli, M.; Serimaa, R.; Nyholm, P.; Ikkala, O. *Macromol. Chem. Phys.* **2002**, *203*, 388.

(52) Allcock, H. R.; Lampe, F. W.; Mark, J. E. *Contemporary Polymer Chemistry*, 3rd ed.; Pearson Education: Upper Saddle River, NJ, 2003; Part 1, Chapter 2.

solution was poured into dishes to evaporate ethanol at room temperature for 5–8 h, followed by heating in an oven at 100 °C for 24 h. The as-made products, transparent films, were scraped from the dishes and crushed into powders. Calcination was carried out in a tubular furnace under an inert atmosphere with a flow rate of 90 cm<sup>3</sup>/min at different temperatures (350–1400 °C) for 2 or 3 h. Two kinds of inert atmospheres were used, argon gas or nitrogen containing a small amount of oxygen (~2.4% in volume, denoted as 2.4% O<sub>2</sub>/N<sub>2</sub>). The heating rate was 1 °C/min below 600 °C and increased to 5 °C/min above 600 °C. The yields of mesoporous polymer resins and carbons heated under 2.4% O<sub>2</sub>/N<sub>2</sub> gas were lower than those under Ar, especially at high calcination temperatures. The mesoporous products calcined under Ar and 2.4% O<sub>2</sub>/N<sub>2</sub> were labeled as FDU-15-*Y* and FDU-15-*YN*, respectively, where *Y* represented the heating temperature. The designation of materials templated by copolymer P123 included P123 inside the brackets at the ends of the names. To remove or decompose the templates, a sulfuric acid-aided extraction method was also used to remove or decompose the templates. For a typical extraction procedure, 1.0 g of as-made FDU-15 products was mixed well with 100 mL of 48 wt % H<sub>2</sub>SO<sub>4</sub> aqueous solution and then heated at 95 °C for 24 h. After washing by ethanol and water, the final product was obtained. This process was repeated again.

**Synthesis of FDU-16 Mesoporous Polymers and Carbons with Cubic Structure (*Im* $\bar{3}m$ ).** FDU-16 mesostructures were templated by using copolymer F127 or F108, with molar compositions in the range of phenol/formaldehyde/NaOH/F127 = 1:2:0.1:0.003–0.008 or phenol/formaldehyde/NaOH/F108 = 1:2:0.1:0.005–0.010. In a typical preparation, 1.0 g of F127 was dissolved in 20.0 g of ethanol, and then 10.0 g of resol precursors in an ethanol solution containing 1.22 g of phenol and 0.78 g of formaldehyde was added under stirring. After 10 min, a homogeneous solution was obtained and was poured into dishes to evaporate ethanol at room temperature for 5–8 h, followed by heating in an oven at 100 °C for 24 h. The as-made and calcined mesoporous products were obtained as described above. They were designated as FDU-16-*Y* or FDU-16-*YN*, where *Y* represents the calcination or carbonization temperature. Where appropriate, the copolymer template is identified within parentheses.

**Synthesis of FDU-14 Mesoporous Polymers and Carbons with Cubic Structure (*Ia* $\bar{3}d$ ).** The synthesis compositions of the FDU-14 mesostructure were in the range of phenol/formaldehyde/NaOH/P123 = 1:2:0.1:0.018–0.019. For a typical synthesis, a homogeneous solution was obtained by mixing a solution of 1.0 g of P123 and 20.0 g of ethanol with 7.5 g of resol precursors in an ethanol solution containing 0.92 g of phenol and 0.58 g of formaldehyde with stirring for 10 min. After the same procedures of solvent evaporation, thermal treatment, and calcination as for FDU-15, the as-made and calcined products were obtained. The final products were designated as FDU-14-*Y* or FDU-14-*YN*, where *Y* represents the heating temperature.

**Synthesis of Lamellar Mesostructured Polymers.** The synthesis was carried out by a similar procedure to that above, using copolymer P123 as a template. The composition was in the range of phenol/formaldehyde/NaOH/P123 = 1:2:0.1:0.022–0.027. In a typical procedure, 1.0 g of P123 was dissolved in 20.0 g of ethanol, and then 5.0 g of resol precursors in an ethanol solution containing 0.61 g of phenol and 0.39 g of formaldehyde was added. With stirring for 10 min, a homogeneous solution was obtained. The solution was poured into dishes to evaporate ethanol at room temperature for 5–8 h, followed by heating in an oven at 100 °C for 24 h. The as-made thick films were peeled off from the dishes and crushed into powders.

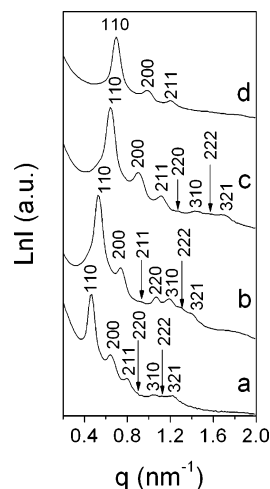


**Figure 1.** SAXS patterns of mesoporous materials FDU-16: as-made FDU-16 (a), that calcined at 350 °C under 2.4% O<sub>2</sub>/N<sub>2</sub> (FDU-16-350N; b), that calcined at 600 °C under Ar (FDU-16-600; c), and that calcined at 1200 °C under Ar (FDU-16-1200; d).

**Synthesis of the Ordered Mesoporous Carbon Replica CMK-3.** The material was prepared according to the procedure given in the literature<sup>53</sup> by using ordered mesoporous silica SBA-15 as a template and sucrose as a carbon precursor. A successive two-step impregnation procedure and high-temperature calcinations at 900 °C under a nitrogen atmosphere were employed. The silica template was etched twice by HF acid.

## Results

**1. Cubic (*Im* $\bar{3}m$ ) Mesostructure (FDU-16).** The mesoporous polymer resin films were deposited by coating the ethanol solution of preformed resols and copolymer templates on glass dishes. The as-made materials are soft and transparent films without cracking, indicating no macroscopic phase separation in the composites of phenolic resins and triblock copolymers. The thickness of the films can be varied from several hundred nanometers to micrometers. Mesoporous polymer FDU-16 can be prepared by using F127 as a template via a solvent EISA method in ethanol solution. The small-angle X-ray scattering (SAXS) patterns of as-made FDU-16 clearly show three well-resolved diffraction peaks with *q* values of 0.47, 0.64, and 0.80 nm<sup>-1</sup> (Figure 1a). Four additional diffraction peaks at *q* values of 0.88, 1.04, 1.12, and 1.22 nm<sup>-1</sup> can also be detected. The *q*-value ratios of these peaks are exactly 1:√2:√3:√4:√5:√6:√7 and can be indexed as 110, 200, 211, 220, 310, 222, and 321 Bragg reflections, respectively, associated with the body-centered cubic *Im* $\bar{3}m$  symmetry.<sup>13</sup> Heating this sample at 350 °C under a 2.4% O<sub>2</sub>/N<sub>2</sub> atmosphere gives a more resolved SAXS pattern, which suggests that the highly ordered cubic mesostructure (*Im* $\bar{3}m$ ) is retained. The calculation from SAXS measurements reflects large unit cell parameters (*a*) of 19.0 and 16.9 nm for as-made FDU-16 and FDU-16-350N, respectively, implying shrinkage (11%) of the framework upon calcination. With further increasing the calcination temperature to 600 °C under an Ar atmosphere, seven resolved SAXS diffraction peaks (Figure 1c) can still be

(53) Jun, S.; Joo, S. H.; Ryoo, R.; Kruk, M.; Jaroniec, M.; Liu, Z.; Ohsuna, T.; Terasaki, O. *J. Am. Chem. Soc.* **2000**, *122*, 10712.

**Table 1. Physicochemical Properties of Mesoporous Polymer Resins and Carbons Prepared Using Triblock Copolymers as Templates via the EISA Method**

sample name	unit cell parameter $a^a$ (nm)	BET surface area <sup>b</sup> (m <sup>2</sup> /g)	micropore area <sup>c</sup> (m <sup>2</sup> /g)	pore size <sup>d</sup> (nm)	pore volume (cm <sup>3</sup> /g)	wall thickness (nm) <sup>e</sup>	molar ratio of C/H/O
as-made FDU-16	19.0 (18.4)						
FDU-16-350N	16.9 (16.2)	460	230	6.6	0.34	8.0	4.4:2.7:1
FDU-16-400N	16.1 (15.3)	670	370	6.1	0.47	7.8	
FDU-16-500	14.6 (14.0)	660	360	4.9	0.42	7.7	
FDU-16-600	13.9 (13.4)	580	400	4.3	0.36	7.7	8.3:2:1
FDU-16-600N	14.5 (14.3)	690	420	4.9	0.44	7.6	
FDU-16-700	13.0 (12.4)	690	480	3.8	0.37	7.5	
FDU-16-800	13.0 (12.5)	820	510	3.8	0.47	7.5	8.6:2:1
FDU-16-800N	13.1 (12.9)	760	510	3.8	0.43	7.5	
FDU-16-900	12.9 (12.4)	740	510	3.8	0.41	7.4	
FDU-16-1200	12.7 (12.3)	990	670	3.8	0.54	7.2	15.4:2:1
FDU-16-1200N	12.8 (12.4)	1490	720	3.8	0.85	7.3	
FDU-16-1400	12.6 (12.1)	990	660	3.5	0.54	7.4	
as-made FDU-16 (F108)	19.0 (17.8)						
FDU-16-600(F108)	12.2 (12.2)	610		2.8	0.32	7.8	
as-made FDU-15	15.9 (15.4)						
FDU-15-350	13.1 (13.2)	430	120	5.4	0.40	7.7	7.0:5.4:1
FDU-15-350N	14.0 (13.5)	640	240	7.1	0.65	6.9	
FDU-15-400	12.2 (11.5)	510	180	4.9	0.41	7.3	
FDU-15-400N	13.4 (12.1)	630	290	6.6	0.59	6.8	
FDU-15-500	11.1 (10.5)	670	340	3.8	0.42	7.3	
FDU-15-600	10.4 (10.1)	590	300	3.1	0.34	7.3	8.2:2.9:1
FDU-15-600N	11.2 (11.1)	750	380	4.9	0.55	6.3	
FDU-15-700	10.0 (9.6)	750	430	3.1	0.42	6.9	
FDU-15-800	9.9 (9.4)	720	410	3.1	0.40	6.8	12.3:2.4:1
FDU-15-800N	10.6 (10.0)	900	510	4.3	0.66	6.3	
FDU-15-900	9.7 (9.4)	650	360	3.1	0.37	6.6	
FDU-15-1200	9.8 (9.7)	730	430	2.8	0.42	7.0	16.6:1.7:1
FDU-15-1200N	9.8 (9.5)	1060	590	3.1	0.59	6.7	
FDU-15-1400	10.1 (9.5)	690	440	2.8	0.61	7.3	
H <sub>2</sub> SO <sub>4</sub> -treated FDU-15	15.7 (15.0)	140	0	7.4	0.26	8.3	
As-made FDU-15(P123)	13.4 (13.4)						
FDU-15-800(P123)	8.7 (8.7)	870	440	2.6	0.47	6.1	
as-made FDU-14	30.0 (26.0)						
FDU-14-350	23.5 (22.8)	130	0	3.1	0.10	6.1	6.6:5.7:1
FDU-14-350N	24.0 (22.8)	280	64	3.9	0.23	5.8	
FDU-14-600	20.0 (18.4)	630	370	2.3	0.32	5.4	
FDU-14-800	20.0 (18.1)	690	470	2.0	0.34	5.5	

<sup>a</sup> Calculated from SAXS results; data in parentheses are calculated from XRD results. <sup>b</sup> Calculated by the BJH model from sorption data in a relative pressure range from 0.04 to 0.2. <sup>c</sup> Calculated by the  $V-t$  method. <sup>d</sup> Calculated by the BJH model from the adsorption branches of the isotherms. <sup>e</sup> Calculated by the formulas  $h = [(\sqrt{3}/2)(a - D)]$ ,  $h = a - D$ , and  $h = (a/3.0919) - (D/2)$  for FDU-16, FDU-15, and FDU-14, respectively, where  $a$  represents the unit cell parameter and  $D$  represents the pore diameter determined by the BJH model.

observed, but with a shift to higher  $q$  values. The calculated unit cell parameter is 13.9 nm. It clearly demonstrates that FDU-16-600 possesses a highly ordered cubic  $Im\bar{3}m$  mesostructure, and the framework continues shrinking at a higher temperature of 600 °C. When the heating temperature is raised to 1200 °C and even 1400 °C (see Figure 1d and Supporting Information, Figure 1), the SAXS patterns show three distinct diffraction peaks assigned to the  $Im\bar{3}m$  symmetry with unit cell parameters of 12.7 and 12.6 nm, respectively (Table 1). This observation suggests that FDU-16 is highly thermally stable, and the framework shrinkage in this temperature range is not as large as that in the range below 600 °C. X-ray diffraction (XRD) patterns (Supporting Information, Figure 2) also illustrate that FDU-16 possesses ordered cubic mesostructures with  $Im\bar{3}m$  symmetry after heating at different temperatures.

The transmission electron microscopy (TEM) images of FDU-16-350N and FDU-16-1200 viewed along the [100], [110], and [111] directions together with the corresponding Fourier diffractograms are shown in Figure 2. They are consistent with the well-ordered body-centered cubic  $Im\bar{3}m$  mesoporous structure. This further demonstrates that FDU-

16 products possess high-quality and large-domain regularity. The cell parameters of FDU-16-350N and FDU-16-1200 estimated from the TEM images are about 16.7 and 12.6 nm, respectively, in good agreement with the results from the SAXS patterns. These results confirm that the ordered mesostructure is highly stable in the temperature range of 350–1400 °C, only undergoing framework shrinkage. Figure 3 displays the N<sub>2</sub> sorption isotherms of calcined FDU-16 materials. After heating at 350 °C under a 2.4% O<sub>2</sub>/N<sub>2</sub> atmosphere, the material shows typical type-IV curves with an obvious H<sub>2</sub>-type hysteresis loop and a sharp capillary condensation step in the  $P/P_0$  range from 0.6 to 0.7, corresponding to a 3-D caged mesostructure with a narrow pore size distribution.<sup>54</sup> The BET surface area, pore volume, and mean pore size are calculated to be 460 m<sup>2</sup>/g, 0.34 cm<sup>3</sup>/g, and 6.6 nm, respectively. The porosity in FDU-16-350N gives evidence of the template decomposition even at a low temperature (350 °C). Notably, the adsorption and desorption isotherms of FDU-16-350N are not closed at the low relative

(54) Matos, J. R.; Kruk, M.; Mercuri, L. P.; Jaroniec, M.; Zhao, L.; Kamiyama, T.; Terasaki, O.; Pinnavaia, T. J.; Liu, Y. *J. Am. Chem. Soc.* **2003**, *125*, 821.

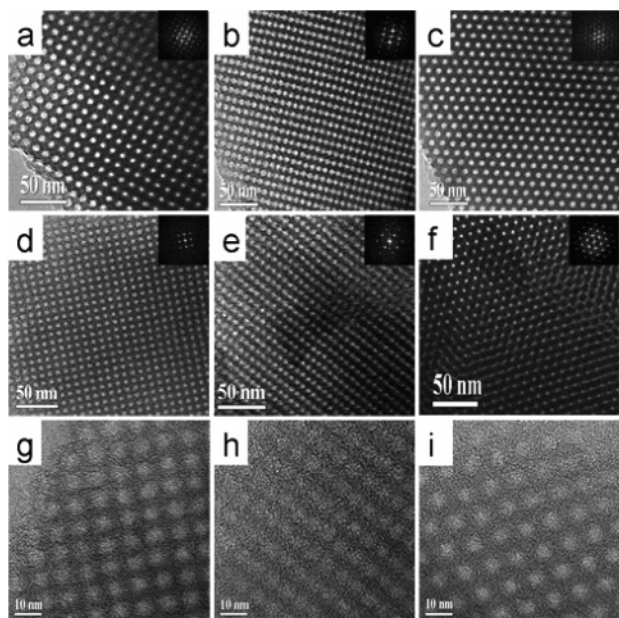


**Figure 2.** TEM images (a–f) and HRTEM images (g–i) of mesoporous materials FDU-16 prepared by using F127 as a template via the EISA method after calcination at 350 °C under 2.4% O<sub>2</sub>/N<sub>2</sub> (FDU-16-350N) (a–c) and at 1200 °C under Ar (FDU-16-1200; d–i), viewed along the [100] (a, d, g), [110] (b, e, h), and [111] (c, f, i) directions. The insets are the corresponding fast Fourier transform (FFT) diffractograms.

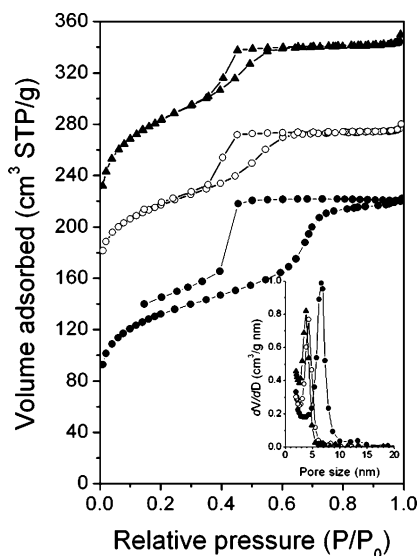


**Figure 3.** Nitrogen sorption isotherms and pore size distributions (inset) of 3-D cubic mesoporous materials FDU-16 prepared by using F127 as a template via the EISA method after calcination at 350 °C under 2.4% O<sub>2</sub>/N<sub>2</sub> (FDU-16-350N; solid circles), at 600 °C under Ar (FDU-16-600; open circles), and at 1200 °C under Ar (FDU-16-1200; solid triangles). The isotherm of FDU-16-600 is offset vertically by 50 cm<sup>3</sup>/g.

pressures, which are typical isotherms of polymers.<sup>55</sup> Calcination at 600 and 1200 °C under Ar yields isotherms similar to those of FDU-16-350N. The difference is the clear capillary condensation steps occurring at the lower relative pressures, which are related to the reduction of pore sizes. Indeed, the mean pore sizes of FDU-16-600 and FDU-16-1200 calculated from the BJH model are 4.9 and 3.8 nm, respectively, which are much smaller than that of FDU-16-

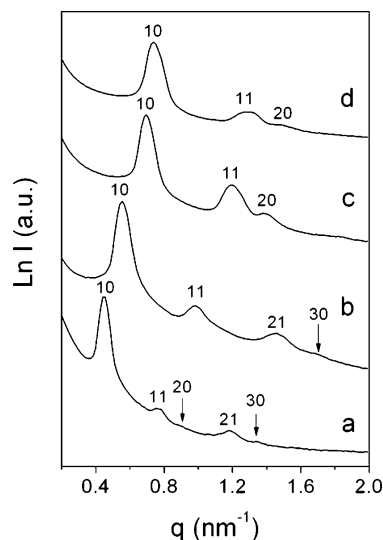


**Figure 4.** SAXS patterns of mesoporous materials FDU-15 prepared by using F127 as a template via the EISA method: as-made FDU-15 (a), that calcined at 350 °C (FDU-15-350; b), that calcined at 600 °C (FDU-15-600; c), and that calcined at 1200 °C (FDU-15-1200; d) under Ar.

350N. On the other hand, the BET surface area of FDU-16-1200 is 990 m<sup>2</sup>/g, much higher than that of FDU-16-350N, suggesting that microporosity is generated. These results further indicate that the cubic mesostructure of FDU-16 is thermally stable.

Resembling cubic mesoporous silica SBA-16 prepared by the use of copolymer F127 with the large PEO/PPO ratio of 3 as the template via the EISA method,<sup>56</sup> body-centered cubic FDU-16 can be synthesized over a wide molar composition range (1.0:2.0:0.1:0.003–0.008 phenol/formaldehyde/NaOH/F127). The evaporation time shows a minor influence on the self-assembly of triblock copolymer and resols due to the slow polymerization rate of resols under neutral conditions at room temperature. Copolymer Pluronic F108 with the large PEO/PPO ratio of 5.3 can also be used as a template to prepare highly ordered FDU-16. The SAXS patterns (Supporting Information, Figure 3) of the as-made and calcined materials prepared with a molar composition of 1.0:2.0:0.1:0.01 phenol/formaldehyde/NaOH/F108 show three well-defined diffraction peaks ascribed to the cubic *Im* $\bar{3}m$  symmetry, indicative of an ordered 3-D mesostructure. The BET surface area and pore volume of mesoporous FDU-16-600(F108) are 610 m<sup>2</sup>/g and 0.32 cm<sup>3</sup>/g, respectively (Table 1). The pore size is calculated to be 2.8 nm, which is smaller than that of FDU-16-600 templated by F127.

**2. 2-D Hexagonal Mesostructure FDU-15.** An ordered mesoporous FDU-15 polymer resin and carbon structure can be synthesized by adding a large amount of F127 template into the synthetic system. The SAXS pattern (Figure 4a) of the as-made samples shows five resolved diffraction peaks. They can be indexed to 10, 11, 20, 21, and 30 planes of a 2-D hexagonal mesostructure (space group *p6m*),<sup>4</sup> which is highly ordered. Upon calcination at different temperatures from 350 to 1200 °C in Ar, the SAXS patterns (Figure 4b–d) become less resolved and the diffraction peaks broaden.

(55) McKeown, N. B.; Budd, P. M.; Msayib, K. J.; Ghanem, B. S.; Kingston, H. J.; Tattershall, C. E.; Makhseed, S.; Reynolds, K. J.; Fritsch, D. *Chem.–Eur. J.* **2005**, *11*, 2610.

(56) Zhao, D.; Yang, P.; Melosh, N.; Feng, J.; Chmelka, B. F.; Stucky, G. D. *Adv. Mater.* **1998**, *10*, 1380.

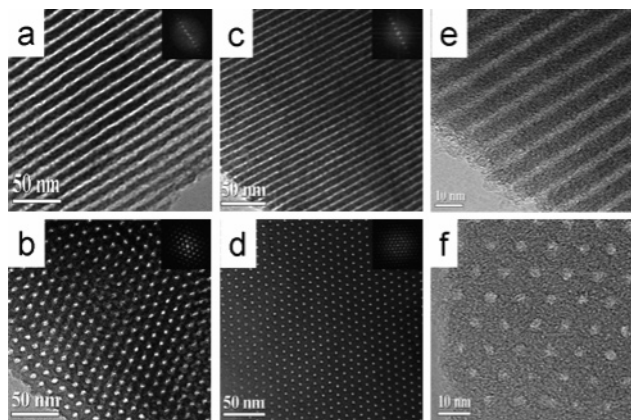


**Figure 5.** TEM images (a–d) and HRTEM images (e, f) of mesoporous materials FDU-15 prepared by using F127 as a template via the EISA method after calcination at 350 °C (FDU-15-350; a, b) and at 1200 °C (FDU-15-1200; c–f) under an Ar atmosphere, viewed from the [110] (a, c, e) and [001] (b, d, f) directions. The insets are the corresponding FFT diffractograms.

However, at least three resolved diffraction peaks can be clearly observed, suggesting that the FDU-15 mesostructure is thermally stable. The  $q$  vectors move to higher values as the calcination temperature increases (Table 1), implying a contraction of the framework. A remarkable breakpoint of framework shrinkage is noted near 600 °C; at higher temperatures, the framework shrinkage becomes lower. The XRD patterns (Supporting Information, Figure 4) also suggest that mesoporous FDU-15 has a highly ordered hexagonal mesostructure, which is thermally stable even at 1400 °C (Supporting Information, Figure 1).

The typical stripe-like and hexagonally arranged TEM images (Figure 5), viewed from the [110] and [001] directions, respectively, are observed in the FDU-15 samples calcined at 350 and 1200 °C, consistent with a high-quality hexagonal mesostructure and thermal stability. The unit cell parameters of FDU-15-350 and FDU-15-1200 estimated from the TEM images are 13.1 and 10.1 nm, respectively, in agreement with the values calculated from the SAXS data.

Figure 6 depicts the N<sub>2</sub> sorption isotherms of FDU-15 samples calcined at different temperatures in Ar gas. Typical type-IV curves with a clear condensation step at  $P/P_0 = 0.6–0.7$  are observed for FDU-15-350, implying a uniform mesopore. However, different from that of FDU-15-350N calcined under 2.4% O<sub>2</sub>/N<sub>2</sub> (see below), the desorption branch of isotherms does not give a good H<sub>1</sub>-type hysteresis loop, implying that the pore channels may be blocked. It may arise from incomplete decomposition of templates in FDU-15 channels under Ar. The adsorption and desorption isotherms of FDU-15-350N are also not closed, attributed to the sample's polymer framework. FDU-15-350 exhibits a large pore size of 5.4 nm, a high BET surface area of 430 m<sup>2</sup>/g, and a pore volume of 0.40 cm<sup>3</sup>/g. Thermal treatment at 600 and 1200 °C yields typical type-IV isotherms with evident capillary condensation steps at lower relative pressures, consistent with the reduction of pore sizes (Table 1). In addition, rather narrow pore size distributions are observed (Figure 6, inset), with mean values of 3.1 and 2.8 nm for FDU-15-600 and FDU-15-1200, respectively (Table 1).

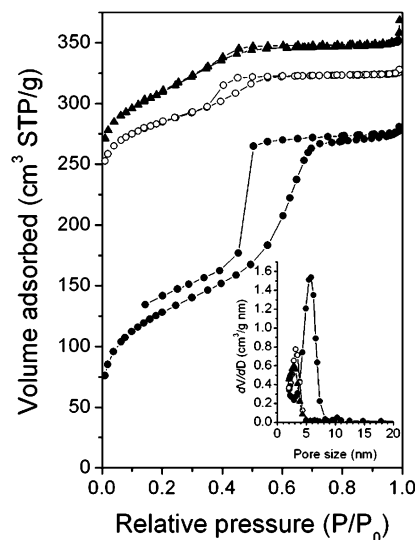


**Figure 6.** Nitrogen sorption isotherms of mesoporous materials FDU-15 prepared by using triblock copolymer F127 as a template via the EISA method after calcination at 350 °C (FDU-15-350; solid circles), at 600 °C (FDU-15-600; open circles), and at 1200 °C (FDU-15-1200; solid triangles) under argon. The inset shows the pore size distributions. Both the isotherms of FDU-15-600 and FDU-15-1200 are offset vertically by 100 cm<sup>3</sup>/g.

Similar to hexagonal mesoporous silica SBA-15,<sup>56</sup> ordered polymer resin and carbon mesostructure FDU-15 can also be templated by Pluronic P123. The XRD pattern (Supporting Information, Figure 5a) of as-made FDU-15 prepared with a molar composition of phenol/formaldehyde/NaOH/P123 = 1:2:0.1:0.013 displays a narrow and intense diffraction peak at a  $2\theta$  value of 0.87°, as well as two resolved diffraction peaks at 1.65 and 2.18°, which can be indexed as the 10, 20, and 21 reflections of a 2-D hexagonal mesostructure.<sup>56</sup> It suggests a periodic regularity of the mesostructure. After calcination at 800 °C under Ar, the intensity of the 10 diffraction peak (Supporting Information, Figure 5b) becomes more intense as a result of the framework contrast after removal of the templates, and the 11 diffraction peak becomes resolved. The N<sub>2</sub> sorption isotherms of FDU-15-800(P123) clearly show representative type-IV curves and reveal a uniform pore size of 2.6 nm (Table 1). Compared with FDU-15-800 templated by Pluronic F127, the cell parameter and pore size of FDU-15-800(P123) are smaller (Table 1). On the basis of our experimental results, Pluronic P123 can direct the synthesis of 2-D hexagonal FDU-15 in a composition range of 1.0:2.0:0.1:0.007–0.016 phenol/formaldehyde/NaOH/P123.

**3. Cubic Bicontinuous Mesostructure FDU-14.** Mesoporous FDU-14 with bicontinuous cubic  $Ia\bar{3}d$  symmetry can be synthesized by using P123 as a template via the EISA method. The SAXS patterns of as-made and calcined FDU-14 materials are shown in Figure 7. Although only two reflection peaks with  $q$  values at 0.58 and 0.60 nm<sup>-1</sup> are observed in the SAXS pattern (Figure 7a) of as-made FDU-14, the  $q$ -value ratio is nearly 0.866. Combined with the results from TEM measurements (see below), the two diffraction peaks are indexed as 211 and 220 reflections of the cubic mesostructure ( $Ia\bar{3}d$ ), respectively.<sup>12</sup> After calcination at 350 °C under 2.4% O<sub>2</sub>/N<sub>2</sub>, in addition, two broad diffraction peaks appear in the  $q$  range from 1.0 to 1.4 nm<sup>-1</sup>, which are attributed to the overlap of 321 and 400 reflections

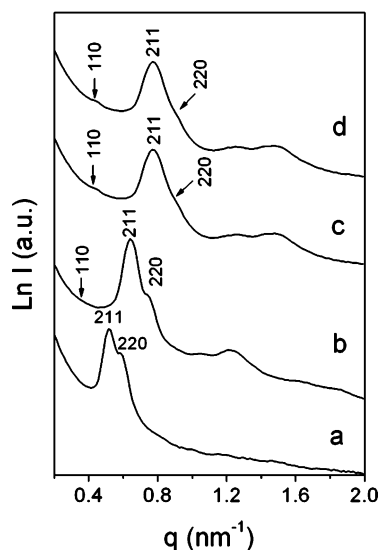


**Figure 7.** SAXS patterns of the bicontinuous mesostructure FDU-14 prepared by using triblock copolymer P123 as a template via the EISA method: as-made FDU-14 (a) and those calcined at 350 °C under 2.4% O<sub>2</sub>/N<sub>2</sub> atmosphere (FDU-14-350N; b), at 600 °C under Ar (FDU-14-600; c), and at 800 °C under Ar (FDU-14-800; d).

and that of 420 and 332 reflections for  $Ia\bar{3}d$  symmetry, respectively. As the calcination temperature rises to 600 and 800 °C under Ar, the 211 and 220 reflection peaks become wide and poorly resolved, suggesting a continuous structural distortion. Similar to our previous observations of FDU-14 prepared by a hydrothermal method,<sup>57</sup> a very weak diffraction peak in the SAXS patterns of calcined FDU-14 materials indexed as the 110 reflection of  $I4_132$  symmetry is detected, implying a small structural defect. The unit cell parameters of as-made FDU-14, FDU-14-350N, FDU-14-600, and FDU-14-800 are calculated to be 30.0, 24.0, 20.0, and 20.0 nm (Table 1), suggesting that the framework shrinkage is large at temperatures lower than 600 °C and decreases in the range above 600 °C. It should be noted that only one intense diffraction peak at the  $2\theta$  value of 0.83° indexed as the 211 diffraction is detected in the XRD patterns of as-made FDU-14 (Supporting Information, Figure 6a) and the 220 diffraction is not resolved. This phenomenon has also been observed in the mesoporous silicate FDU-5<sup>12</sup> with  $Ia\bar{3}d$  structure prepared via the EISA process. After calcination, a broad diffraction peak at  $2\theta$  values ranging from 1.2 to 2.6 appears (Supporting Information, Figure 6b–d), arising from the overlap of 321, 400, 420, and 332 diffraction peaks of  $Ia\bar{3}d$  symmetry.

Figure 8 shows the TEM images and the corresponding Fourier diffractograms of FDU-14-350N and FDU-14-600 recorded along the [531], [100], [111], and [331] directions. The highly ordered arrangements of the mesopores further reveal that the FDU-14-350N products possess the cubic bicontinuous mesostructure. After calcination at 600 °C under Ar, large domains of the ordered  $Ia\bar{3}d$  mesostructure can still be observed, suggesting thermal stability. Although a weak 110 reflection is detected in the SAXS patterns, no typical patterns of  $I4_132$  symmetry are observed in the TEM images, implying that the main phase of the FDU-14 products has

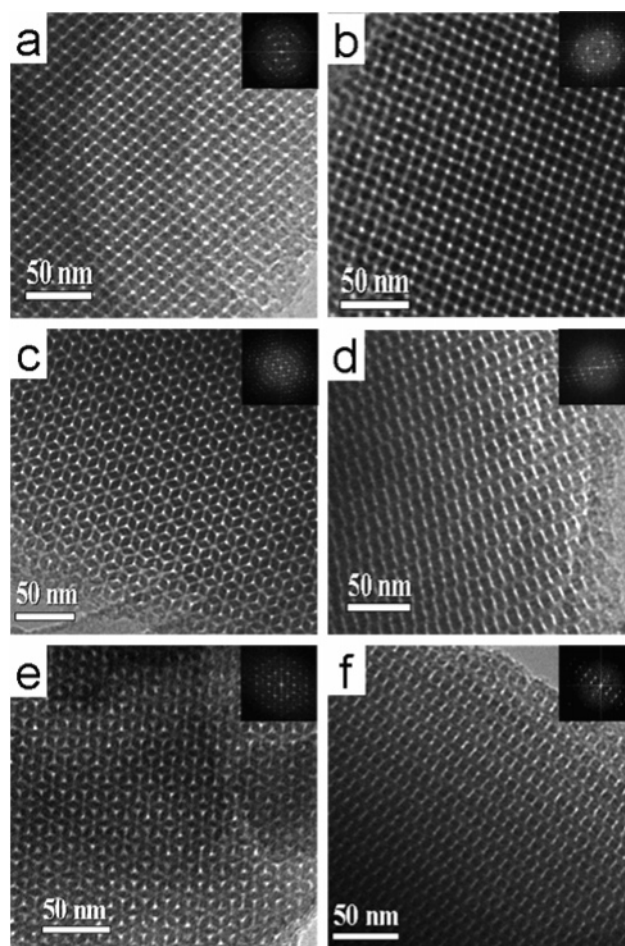


**Figure 8.** TEM images of mesoporous materials FDU-14 prepared by using triblock copolymer P123 as a template via the EISA method: that calcined at 350 °C under N<sub>2</sub> (FDU-14-350N; a–d) and calcined FDU-14 at 600 °C (e, f) under Ar (FDU-14-600), viewed along the [531] (a), [100] (b), [111] (c, e), and [331] (d, f) directions. The insets are the corresponding FFT diffractograms.

the  $Ia\bar{3}d$  symmetry. Estimated from the TEM images, the cell parameters ( $a$ ) of FDU-14-350N and FDU-14-600 are 23.7 and 19.8 nm, respectively, coincident with the results from the SAXS patterns.

The N<sub>2</sub> sorption isotherms (Figure 9) illustrate that calcined FDU-14 materials have typical type-IV curves and capillary condensation steps, suggesting uniform mesopores. The FDU-14-350N sample calcined at 350 °C in 2.4% O<sub>2</sub>/N<sub>2</sub> shows capillary condensation at relative pressures of 0.4–0.65. A narrow pore size distribution with a mean value of 3.9 nm (Figure 9, inset) can be calculated from the BJH model. Similar to those of FDU-16-350N, open adsorption and desorption isotherms obviously appear, which is related to the organic property of the polymer framework.<sup>55</sup> An unusual H<sub>2</sub>-type hysteresis is observed in FDU-15-350N, unlike that of mesoporous silica FDU-5 (space group  $Ia\bar{3}d$ ) with a large pore of 8 nm<sup>12</sup> which may be due to the smaller pore size around 4 nm of the former. FDU-14-350N has a BET surface area of 280 m<sup>2</sup>/g and a pore volume of 0.23 cm<sup>3</sup>/g. After heating at 600 °C under Ar, FDU-14-600 exhibits a capillary condensation in N<sub>2</sub> sorption isotherm curves with a shift to low relative pressure, which is similar to small pore mesoporous silica MCM-48.<sup>2</sup> The pore size is reduced to 2.3 nm, while the BET surface area

(57) Zhang, F. Q.; Meng, Y.; Gu, D.; Yan, Y.; Yu, C. Z.; Tu, B.; Zhao, D. Y. *J. Am. Chem. Soc.* **2005**, *127*, 13508.



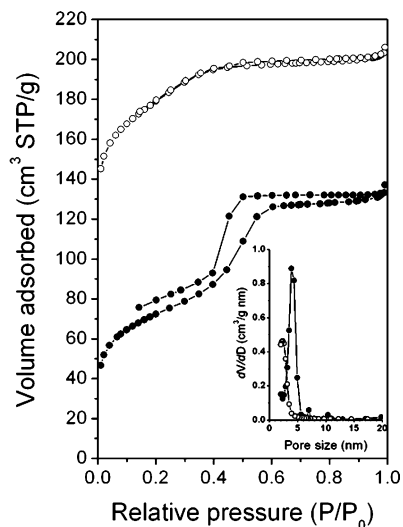


**Figure 9.** Nitrogen sorption isotherms and pore size distributions (inset) of mesoporous materials FDU-14 prepared by using triblock copolymer P123 as a template via the EISA method after calcination at 350 °C under 2.4% O<sub>2</sub>/N<sub>2</sub> (FDU-14-350N; solid circles) and at 600 °C under Ar (FDU-14-600; open circles).

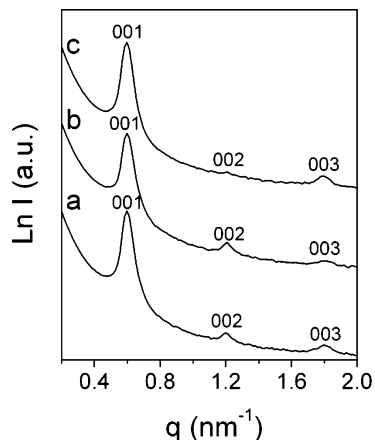


**Figure 10.** SAXS patterns of as-made lamellar mesostructure with P123/phenol molar ratios of 0.022:1 (a), 0.025:1 (b), and 0.027:1 (c).

and pore volume increase to 630 m<sup>2</sup>/g and 0.32 cm<sup>3</sup>/g, respectively.

Different from syntheses of mesoporous silicate with 3-D bicontinuous structure (*Ia3d*) templated from copolymer P123, which require various kinds of additives such as 3-mercaptopropyltrimethoxy silane<sup>12</sup> or *n*-butanol,<sup>58</sup> FDU-14 can be derived by simply raising the P123 concentration in the synthetic system. However, by using an EISA method with a copolymer P123 template, the FDU-14 mesostructure can only be synthesized in a very narrow range with the composition of 1.0:2.0:0.1:0.018–0.019 phenol/formaldehyde/NaOH/P123.

**4. Lamellar Mesostructure.** When further increasing the P123 concentration to the phenol/P123 molar ratio of 1:0.022, lamellar mesostructured polymers can be prepared as shown in the SAXS patterns (Figure 10a). Three well-resolved diffraction peaks with *q*-value ratios of 1:2:3 appear, associated with the lamellar mesostructure (*Lα*). Interestingly, the intense 001 peak reflects a *d* value of 10.5 nm, consistent with that of the 220 diffraction peak in as-made FDU-14. It

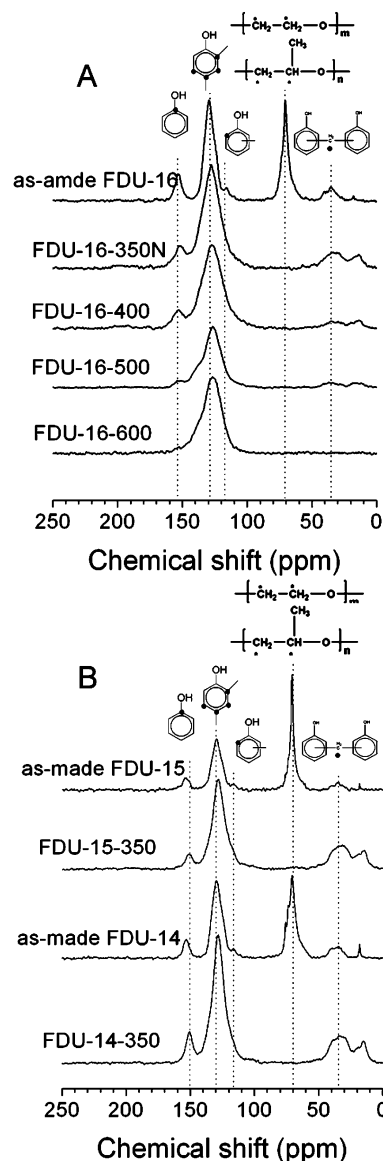


**Figure 11.** Solid state <sup>13</sup>C CP-MAS NMR spectra of (A) as-made FDU-16, FDU-16-350N, FDU-16-400, FDU-16-500, and FDU-16-600 and (B) as-made FDU-15, FDU-15-350, as-made FDU-14, and FDU-14-350.

may give a hint about the phase transition from lamellar to *Ia3d* mesostructure. The SAXS patterns (Figure 10b,c) of the mesostructured polymers almost remain the same as the synthetic molar ratio of phenol to P123 decreases to 1:0.027, indicating that the ordered lamellar mesostructure can be formed in this range (1.0:2.0:0.1:0.022–0.027 phenol/formaldehyde/NaOH/P123). However, the lamellar mesostructure is not stable. Attempts to remove the template upon calcination at temperatures ranging from 350 to 800 °C failed.

**5. Framework Constitution.** To elucidate the composition and structure of the frameworks, an elaborate study was carried out by the combination of NMR, Fourier transform infrared (FT-IR), and elemental analyses. <sup>13</sup>C cross-polarization magic angle spinning (CP-MAS) NMR spectra of the as-made and mesoporous materials calcined at 350 °C are presented in Figure 11. The as-made products show two strong and broad signals with chemical shifts around 153 and 130 ppm (Figure 11), which are attributed to the OH-substituted carbon in phenol and other aromatic carbons

except for the OH-substituted aromatic carbon, respectively.<sup>59</sup> A shoulder peak at 120–110 ppm can be assigned to nonsubstituted aromatic ortho carbons.<sup>59</sup> The broad overlapping signals at around 36 ppm can be ascribed to methylene linkages between phenolic rings.<sup>59</sup> An intense and narrow peak at around 70 ppm, corresponding to the carbons in the copolymer F127 or P123 template,<sup>15</sup> is observed for all as-made samples. These results illustrate that the as-made networks are hybrid composites of phenolic resins and amphiphilic copolymers. Obvious differences are observed in the <sup>13</sup>C NMR spectra (Figure 11) of the calcined materials. The signal at 70 ppm disappears, implying that almost all of triblock copolymer templates are decomposed and removed, in accordance with the nitrogen sorption results. The weak shoulder signal at 120–110 ppm is barely visible, suggesting that phenolic resins further cross-link during the thermal treatment at 350 °C. The preservation of the residual four resonances further suggests the presence of polymeric frameworks. As the calcination temperature increases, the <sup>13</sup>C NMR spectra (Figure 11) show that the intensities of the characteristic resonance peaks at 153, 130, 120–110, and 36 ppm continuously decrease. After calcination at 600 °C, these peaks are hard to see. The reservation of the chemical shift at 130 ppm may be related to the carbon framework.<sup>60</sup> These results imply that framework constituents have changed. Elemental analyses (Table 1) reveal that the molar ratios of C/H/O in FDU-15-350 and FUD-14-350 calcined at 350 °C under Ar are close to that in the ideal cross-linked phenolic resin (C/H/O = 7:5:1), indicating that the mesoporous materials prepared by using organic–organic self-assembly are made of phenolic resin polymer frameworks. But the molar ratio of C/H/O in FDU-16-350N (Table 1) is smaller than 7:5:1, suggesting that the content of elemental O is higher than those in FDU-15-350 and FDU-14-350. This result is attributed to the presence of oxygen during calcination, which erodes the hydrocarbon species on the wall. A low carbon content and high hydrogen and oxygen contents for the calcined products at temperatures of 350–600 °C (Table 1) suggest that the frameworks resemble resin polymers. The wide-angle XRD patterns (data not shown) reveal that the polymer frameworks are amorphous.

The FT-IR spectrum of the as-made FDU-16 shows a strong but rather broad band at ~3400 cm<sup>-1</sup> arising from –OH stretching (Figure 12a), suggesting the existence of a large amount of phenolic –OH group and un-cross-linked benzyl alcohol. The broadness of the absorption arises from intermolecular H-bonding. The band at 1610 cm<sup>-1</sup> is caused by carbon–carbon bond stretching of 1,2,4- and 1,2,6-trisubstituted and phenyl alkyl ether-type substituted aromatic ring structures,<sup>61,62</sup> implying the framework of as-made FDU-16 is that of network phenolic resins. Several bands at 1100 and 2800–3000 cm<sup>-1</sup> can be assigned to the C–O and C–H stretching of copolymer F127. After calcination at 350 °C under 2.4% O<sub>2</sub>/N<sub>2</sub> (Figure 12b), the bands at 1100 and 2800–

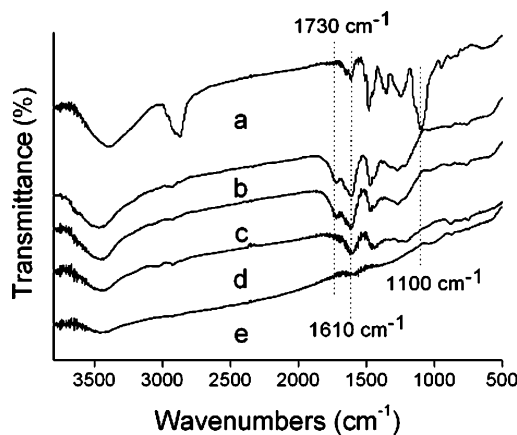


**Figure 12.** FT-IR spectra of cubic mesoporous material FDU-16 prepared by using triblock copolymer P127 as a template via the EISA method: as-made FDU-16 (a) FDU-16-350N (b), FDU-16-400 (c), FDU-16-500 (d), and FDU-16-600 (e).

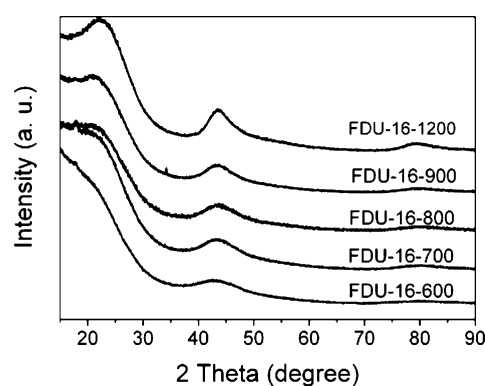


**Figure 13.** Wide-angle XRD patterns of cubic mesoporous carbon FDU-16 calcined at 600, 700, 800, 900, and 1200 °C under Ar.

3000 cm<sup>-1</sup> almost disappear, further giving evidence of template decomposition and removal. A new band at 1730 cm<sup>-1</sup> caused by the vibration of tetra-substituted benzene rings<sup>61,62</sup> is observed, suggesting that the cross-linking degree of phenolic resins improves during the heat treatment. As the heating temperature rises, the FT-IR spectra (Figure 12c–e) show that the relative intensities of all characteristic bands discussed above decrease and almost disappear above 600 °C. The disappearance of the FT-IR vibration bands clearly indicates the variation of the framework constitutions, coincident with the NMR results and thermogravimetric behavior (see below). Indeed, higher carbon contents than in FDU-16-350N are detected in the mesoporous material heated at 600 °C (Table 1).

Figure 13 displays the wide-angle XRD patterns of FDU-16 calcined at different temperatures under Ar. FDU-16-600 shows a weak diffraction shoulder at  $2\theta \sim 23^\circ$ , together with a broad diffraction peak at about  $43^\circ$ , corresponding to 002 and 10 reflections of carbon materials.<sup>63</sup> These data suggest that the framework is composed of carbon. The two diffraction peaks become more resolved with increasing temperature. Simultaneously, elemental analyses show that the carbon contents increase, whereas the oxygen and hydrogen contents diminish (Table 1). It indicates that the

(59) GrenierLoustalot, M. F.; Larroque, S.; Grenier, P. *Polymer* **1996**, *37*, 639.

(60) Zhang, X. Q.; Solomon, D. H. *Chem. Mater.* **1999**, *11*, 384.

(61) Kim, Y. J.; Kim, M. I. I.; Yun, C. H.; Chang, J. Y.; Park, C. R.; Inagaki, M. *J. Colloid Interface Sci.* **2004**, *274*, 555.

(62) Trick, K. A.; Saliba, T. E. *Carbon* **1995**, *33*, 1509.

(63) Yang, H. F.; Yan, Y.; Liu, Y.; Zhang, F. Q.; Zhang, R. Y.; Meng, Y.; Li, M.; Xie, S. H.; Tu, B.; Zhao, D. Y. *J. Phys. Chem. B* **2004**, *108*, 17320.

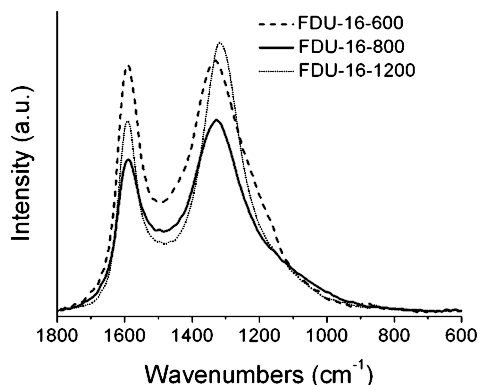


**Figure 14.** Raman spectra of FDU-16 prepared by using triblock copolymer F127 as a template via the EISA method after calcination at 600 °C (dashed line), 800 °C (solid line), and 1200 °C (dotted line) under Ar.

degree of framework carbonization is enhanced as the temperature increases. The XRD patterns are characteristic of amorphous carbon even after carbonization at 1200 °C, suggesting a difficult graphitization of the frameworks.<sup>45</sup> This may be related to the carbon precursor of phenolic resins and the low calcination temperature.

The Raman spectra of calcined FDU-16 (Figure 14) show a broad peak at 1330  $\text{cm}^{-1}$  corresponding to the D band that overlaps with the G band at 1600  $\text{cm}^{-1}$ , indicative of a glassy carbon framework.<sup>45</sup> Increasing the calcination temperature does not cause a distinct change in the Raman spectra (Figure 14), characteristic of amorphous carbon. No large domain of graphitic structure is found in the high-resolution TEM (HRTEM) images (Figure 2g–i) of FDU-16-1200, further confirming that the carbon frameworks are amorphous.

Similar observations are given in the FT-IR spectra (Supporting Information, Figure 7), elemental analyses (Table 1), HRTEM images (Figure 5e,f), wide-angle XRD patterns (Supporting Information, Figure 8), and Raman spectra (Supporting Information, Figure 9) of mesoporous FDU-15. These results suggest that the frameworks possess organic polymer properties after heating at 350–500 °C and can be transformed to amorphous carbon network structures above 600 °C.

**6. Removal of the Template.** In view of the different reactivities of triblock copolymer templates and phenolic resins, two methods can be utilized to efficiently decompose and/or remove the templates while generating ordered mesopores and maintaining an open framework. One is simple heating treatment, and another is solvent extraction. Thermogravimetric analysis (TGA) was employed to monitor the degradation behavior of as-made products and copolymer templates in a  $\text{N}_2$  atmosphere. Notable weight losses of approximately 97.5, 98.8, and 96.8% (Figure 15) are observed in the temperature range of 300–400 °C for pure copolymers F127, P123, and F108, respectively, suggesting that most of the templates can be decomposed even under  $\text{N}_2$  at 400 °C. Three detectable weight loss steps appear in the TGA curves (Figure 15) of all the as-made products. The large weight loss occurs in the range of 300–400 °C, which is mainly attributed to the degradation of templates. Combined with the above  $\text{N}_2$  sorption, SAXS (XRD),  $^{13}\text{C}$  NMR, FT-IR, and elemental analysis measurements, these results clearly indicate that the copolymer templates can be decom-

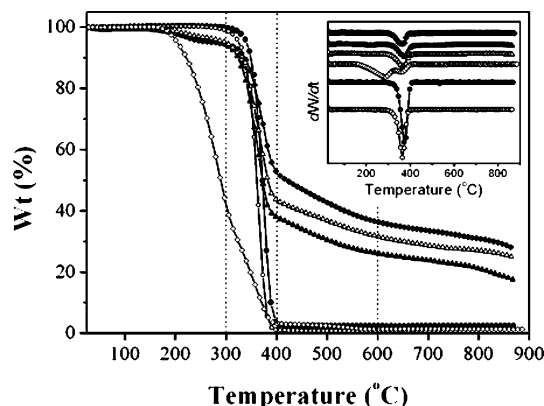


**Figure 15.** TGA and differential thermogravimetry curves (inset) of triblock copolymers F127 (solid circles), P123 (open circles), F108 (open diamonds), as-made FDU-16 templated by F127 (solid diamonds), as-made FDU-15 templated by F127 (solid triangles), and as-made FDU-14 templated by P123 (open triangles).

posed by simple calcination at 300–400 °C under  $\text{N}_2$  to generate mesoporous polymer resin frameworks. The weight losses between 400 and 600 °C as well as above 600 °C coincide with the shrinkage of the frameworks. However, the former weight loss is about 15% while the latter is very little, reflecting a change in the framework constitutions at the temperature of 600 °C.

Interestingly, the template removal is greatly influenced by the presence of oxygen in the feed gas. The triblock copolymer templates in both bicontinuous cubic FDU-14 and 2-D hexagonal FDU-15 mesostructures can be easily removed by calcination at 350 °C under inert argon gas without detectable oxygen, as evidenced by the porosity shown in Table 1. SAXS (or XRD) patterns and TEM images confirm the reserve of highly ordered mesostructure for FDU-14 and FDU-15. Although the templates in the body-centered ( $Im\bar{3}m$ ) FDU-16 mesostructure can also be decomposed upon calcination under argon at 350 °C based on the NMR and FT-IR results,  $\text{N}_2$  sorption isotherms show that it has no porosity and a very low BET surface area of approximately 25  $\text{m}^2/\text{g}$ . It clearly indicates that the caged-like mesopores are not open.

When nitrogen gas containing a small amount ( $\sim 2.4\%$ , v/v) of oxygen is fed into the tube furnace, the large porosity of FDU-16 can be acquired after calcination at 350 °C (Figure 3) and the ordered cubic mesostructure can be preserved, based on the above-mentioned SAXS (XRD) and TEM measurements. These results clearly show that a small amount of oxygen favors opening of the cage windows of mesopores. Compared to isotherms of FDU-15-350 (Figure 6a), the  $\text{N}_2$  isotherms of FDU-15-350N calcined at 350 °C under 2.4%  $\text{O}_2/\text{N}_2$  (Figure 16) reveal a much sharper capillary condensation step at a higher relative pressure of  $\sim 0.7$  and a more perfect  $\text{H}_1$ -type hysteresis loop. This indicates that FDU-15-350N possesses a more ideal cylindrical channel with a bigger pore size,<sup>4</sup> a higher pore volume, and a larger BET surface area (Table 1). Three well-resolved diffraction peaks are observed in the XRD pattern of FDU-15-350N (Figure 17a), suggesting that a small amount of oxygen in the inert gas does not destroy the regularity of the mesostructures. However, the 10 diffraction peak of FDU-15-350N is narrower and more intense than that of FDU-15-350

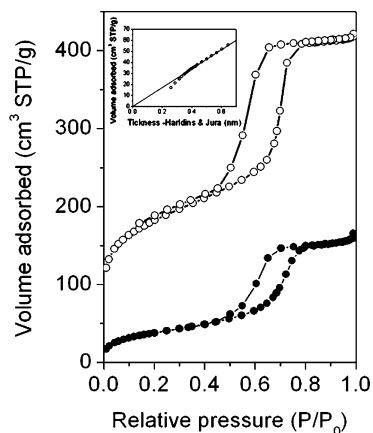


**Figure 16.**  $N_2$  sorption isotherms of FDU-15 prepared by using triblock copolymer F127 as a template via the EISA method refluxed by 48 wt %  $H_2SO_4$  solution (solid circles) and heated at 350 °C under 2.4%  $O_2/N_2$  atmosphere (open circles). The upper inset is the  $t$ -plot curve of 48 wt %  $H_2SO_4$ -treated FDU-15.

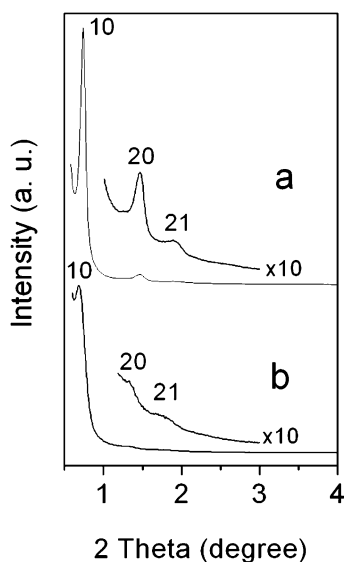


**Figure 17.** XRD patterns of FDU-15 prepared by using triblock copolymer F127 as a template via the EISA method after calcination at 350 °C under 2.4%  $O_2/N_2$  atmosphere (FDU-15-350N) (a) and refluxed with 48 wt %  $H_2SO_4$  solution (b).

calcined under Ar at 350 °C (Supporting Information, Figure 4b), implying that the mesostructure regularity is somewhat improved by the small amount of oxygen in inert gas. Remarkably, the introduction of oxygen can be used at higher temperatures even up to 1200 °C without destroying the mesostructures. Although obtained in lower yield, the products have a slightly larger pore size and higher pore volume and BET surface areas than those calcined under argon at the same temperatures (Table 1). For example, FDU-15-1200N has a BET surface area as high as 1490  $m^2/g$ .  $t$ -plot analysis reveals that the higher BET surface area and pore volume result mainly from microporosity, caused by the oxidation of polymer or carbon species. However, the oxygen content is limited to 3%. Excessive oxygen will burn the frameworks off at a temperature above 700 °C (no solid could be obtained). Therefore, the heating atmosphere has a great influence on the degradation of templates in various mesostructures and the formation of porosities.

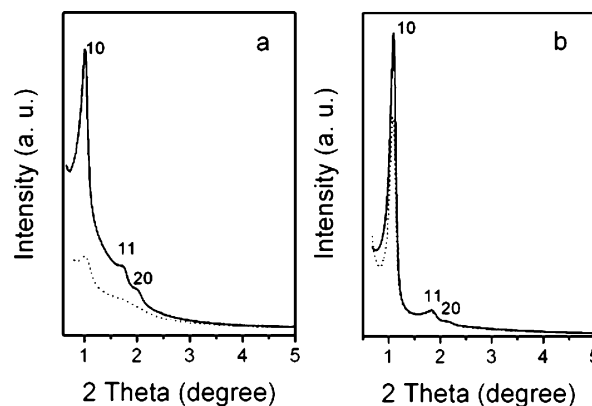


**Figure 18.** XRD patterns of mesoporous carbon (CMK-3) replicated from a mesoporous silica SBA-15 as hard template (left) and mesoporous carbon frameworks FDU-15-900 prepared by using triblock copolymer F127 as a template via the EISA method after calcination at 900 °C under  $N_2$  atmosphere (right). The solid line and the dashed line represent XRD patterns of samples before and after being compressed at 500 MPa for 10 min, respectively.

An alternative method involves solvent extraction with the aid of 48 wt % sulfuric acid to remove and/or decompose the copolymer template. This method has been employed successfully to remove P123 in mesostructured silica SBA-15.<sup>15</sup> Figure 16 shows the  $N_2$  isotherms of FDU-15 refluxed with sulfuric acid at 95 °C for 24 h, which demonstrate type-IV curves with a sharp capillary condensation at  $P/P_0 = 0.7-0.8$  and a typical  $H_1$ -type hysteresis loop, suggesting a yield of uniform mesopore channels. The pore volume and BET surface area of  $H_2SO_4$ -treated FDU-15 are 0.26  $cm^3/g$  and 140  $m^2/g$ , which are much smaller than those of calcined samples (FDU-15-350 or FDU-15-350N). It is noted that the extrapolation of the  $t$ -plot for the former intercepts the y axis close to the origin, indicative of almost no microporosity (Figure 16, inset). The result suggests that the smaller surface area and pore volume may be related to the low microporosity. However,  $H_2SO_4$ -treated FDU-15 possesses a larger pore size of 7.4 nm, perhaps due to the little shrinkage of the frameworks. The XRD pattern of  $H_2SO_4$ -treated FDU-15 (Figure 17b) shows one intense and two weak diffraction peaks, corresponding to the ordered 2-D hexagonal mesostructures. The calculated cell parameter is 15.7 nm, which is nearly equal to that (15.9 nm) of as-made FDU-15. It confirms further a very limited structural shrinkage (1%) after removal of the templates. The results illustrate that the  $H_2SO_4$ -extraction method is much milder than calcination at a high temperature. Unfortunately, it is not suitable for cubic  $Im\bar{3}m$  FDU-16 and  $Ia\bar{3}d$  FDU-14 mesostructures, for which refluxing with sulfuric acid did not produce open mesopores.

**7. Mechanical Stability.** The mechanical stability of mesoporous carbon products was investigated by pressing the material for 10 min at a pressure of 500 MPa. For comparison, replicated mesoporous carbon CMK-3 prepared by using sucrose as a carbon source and SBA-15 as a hard template was also evaluated. The XRD pattern of CMK-3 after compression (Figure 18a) shows a substantial reduction in the intensities, implying a mechanical instability. However, mesoporous carbon FDU-15-900 subjected to the same pressure exhibits little change in the XRD pattern (Figure 18b). This indicates that FDU-15-900 has a higher mechan-

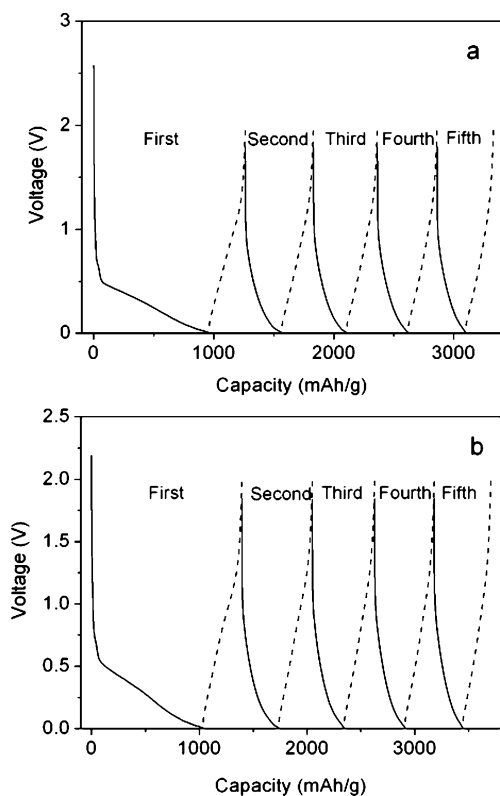


**Figure 19.** Initial five galvanostatic discharge/charge cycles of (a) FDU-15-600 and (b) FDU-16-600 at a constant current of 35 mA/g. Solid and dashed lines represent discharge and charge processes, respectively.

ical stability in comparison with CMK-3, which may be attributed to the continuous framework of the former.

**8. Electrochemical Properties.** The electrochemical properties of mesoporous carbon products as anode materials for lithium-ion batteries were explored. Figure 19 shows the typical galvanostatic charge/discharge curves of mesoporous carbons at a constant current of 35 mA·h/g. It can be seen that the first discharging (reduction) process represents a large specific capacity of  $\sim 962$  mA·h/g for FDU-15-600. However, the reversible capacity (oxidation) in the first process, denoted as  $C_{\text{re}}$ , gives about 300 mA·h/g. It indicates a large loss of capacity, namely, an irreversible capacity  $C_{\text{irr}}$ , of 662 mA·h/g. A large irreversible capacity (350 mA·h/g) in the first cycle of galvanostatic charge/discharge behavior is also detected in the case of cubic mesoporous carbon FDU-16-600, which is a little higher than that of hexagonal FDU-15-600. This fact can, at least partially, be accounted for the well-connected cubic mesostructure that facilitates the diffusion of lithium ion. The Coulombic efficiencies of FDU-15-600 and FDU-16-600 are 31 and 35% in the first cycle, respectively, and soon achieve near 100% in the subsequent cycles. The low Coulombic efficiency in the first cycle is possibly due to the formation of a solid electrolyte interface on the large surface of mesoporous carbons.<sup>64</sup> Despite the large capacity losses in the first cycle of galvanostatic charge/discharge behavior, the reversible capacities of mesoporous carbons exceed those of some carbon nanotubes, that is, 100–1000 mA·h/g, reported elsewhere.<sup>65,66</sup> Notably, FDU-

16-600 displays a comparable reversible capacity with the commercial graphite materials (372 mA·h/g). The reasonably high reversible capacity may be attributed to the integrity of the carbon framework, thick pore walls (6–8 nm), and large pore sizes of FDU-15-600 and FDU-16-600.<sup>64</sup>

## Discussion

**1. Synthesis.** Highly ordered mesoporous polymer resin and carbon materials can be synthesized by organic–organic self-assembly using triblock copolymers as templates via the EISA method. The synthesis procedure includes five major steps (Figure 20): resol precursor preparation, the formation of an ordered hybrid mesophase by organic–organic self-assembly during the solvent evaporation, thermopolymerization of the resols around the template to solidify the ordered mesophase, template removal, and carbonization.

*a. Resol Precursor.* In our case, the choice of organic precursors is essential for the EISA of the organic–organic templating process. Sanchez and co-workers reported<sup>49</sup> that the polymerization degree of inorganic precursors should be low enough to form a moldable inorganic–organic framework at the initial assembly stage of inorganic species with organic surfactants. Highly ordered mesostructures can then be formed. The inorganic framework is “rigid”. Therefore, the mesophase can be solidified, and the surfactant can be easily removed by calcination. In fact, it is the selection of resol, a kind of low-molecular-weight and soluble phenolic resin, as the organic precursor that is the characteristic of this work and also the key issue for successful synthesis of an ordered mesoporous polymer resin and carbon structures.

It is well-known that the polymerization of phenol with formaldehyde can be catalyzed by an acid or a base.<sup>67</sup> The choice of catalyst affects the resulting frameworks. Base-catalyzed processes can result in phenolic resins with a 3-D network structure with benzene rings as three or four cross-linking sites. In contrast, acid catalysts induce linear polymerization according to previous reports.<sup>67</sup> The <sup>13</sup>C NMR spectra (Supporting Information, Figure 11) of resol precursors are characteristic of condensed and substituted phenol groups,<sup>59</sup> suggesting the formation of a tri- or tetra-substituted benzene ring and plenty of benzyl hydroxyl groups besides phenolic hydroxyl groups. It is, therefore, reasonable to choose a base medium for the preparation of the resol precursors. In an ideal network of phenolic resin, one benzene ring links via covalent bonds with three other benzene rings through an aliphatic or an ether bridge. The four-connected benzene rings indeed exist in the framework of the mesoporous polymer products, evidenced by the FT-IR, elemental analysis, and NMR results. Interestingly, this kind of cross-linked structure is similar to that of covalently bonded silicate zeolite frameworks, in which one silicon atom is linked to four other silicon atoms through Si–O bonds. Upon calcination at temperatures lower than 400 °C to remove the template, the “rigid” mesostructure constructed by covalent

(64) Lee, K. T.; Lytle, J. C.; Ergang, N. S.; Oh, S. M.; Stein, A. *Adv. Funct. Mater.* **2005**, *15*, 547.

(65) Frackowiak, E.; Gautier, S.; Gaucher, H.; Bonnamy, S.; Beguin, F. *Carbon* **1999**, *37*, 61.

(66) Frackowiak, E.; Beguin, F. *Carbon* **2002**, *40*, 1775.

(67) Knop, A.; Pilato, L. A. *Phenolic Resins*; Springer: Berlin, 1985.

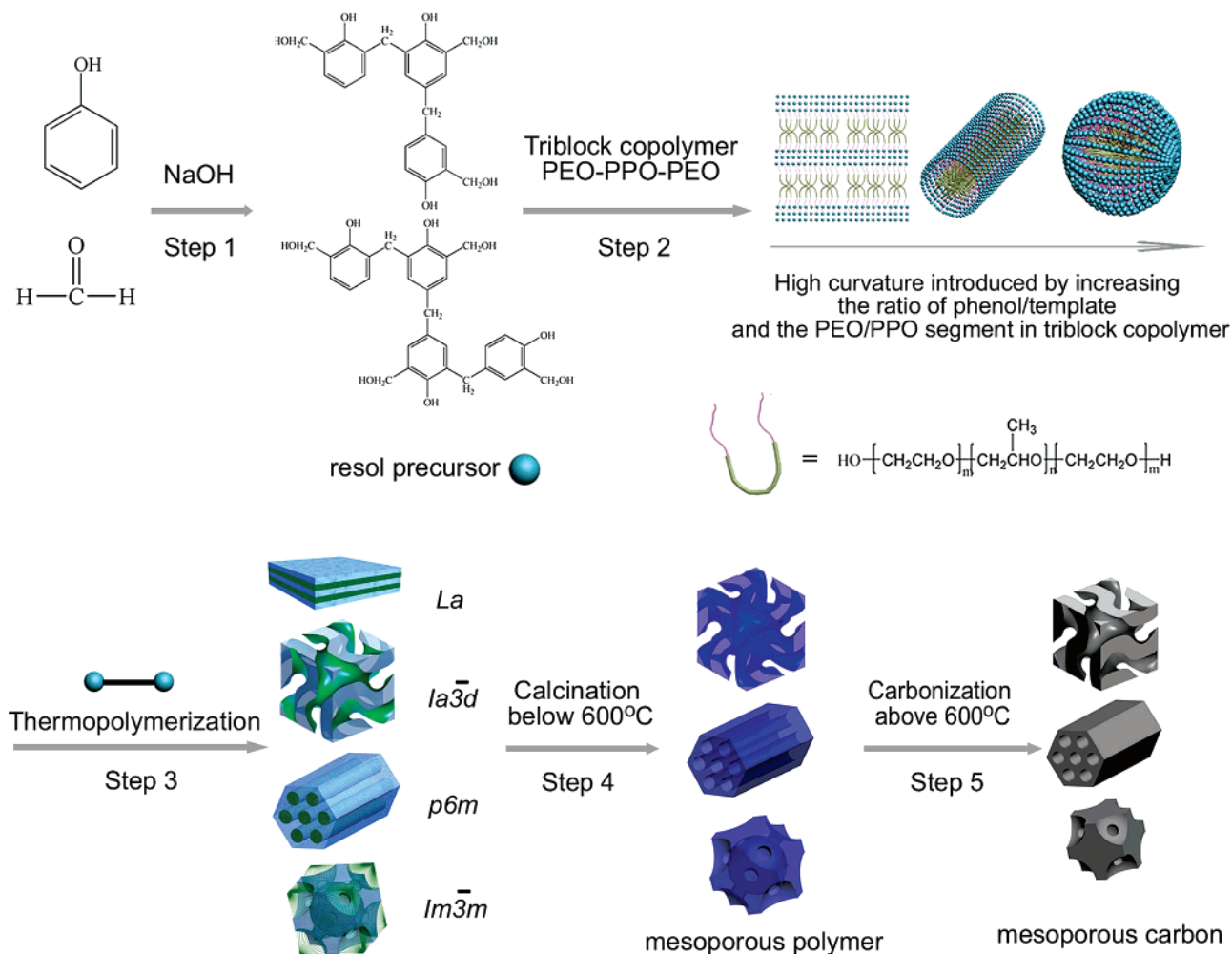


**Figure 20.** Scheme for the preparations of the ordered mesoporous polymer resins and carbon frameworks.

bonds can, therefore, be preserved. Simultaneously, basic conditions facilitate the formation of resol with many benzyl hydroxyl groups besides phenolic hydroxyl groups proved by the  $^{13}C$  NMR spectra (Supporting Information, Figure 11). The interaction can then be generated by abundant hydroxyl groups with the PEO blocks of copolymer PEO–PPO–PEO templates via hydrogen bonds, which favor the assembly of ordered mesostructures. The abundance of benzyl hydroxyl groups and non-substituted ortho carbons on benzene rings provides a chance for resol precursors to cross-link each other with covalent bonds.

The resols are simply prepared from phenol and formaldehyde. Phenol is cheaper than resorcinol, which was previously used.<sup>45,46</sup> Most importantly, the phenol has fewer reactive sites which are more inert than those in resorcinol. Therefore, the polymerization rate of resols is more easily controlled. Compared with the resorcinol/formaldehyde system, the choice of the resols decreases the interaction between the polymer resin precursors themselves; as a consequence, the assembly of phenolic resins and copolymer templates takes place more readily to form ordered mesostructures without macrophase separation. An expensive additive such as EOA<sup>46</sup> is not necessary.

GPC measurements reveal that the resol precursors polymerized under basic conditions have a low molecular weight ( $M_w = 200–500$ ). However, it does not greatly

influence the assembly of mesostructures, because the resols are stable at neutral medium (pH  $\sim 7$ ) and difficult to polymerize further at room temperature. Our results show that resols with molecular weights in the range of 200–5000 are suitable precursors for the synthesis of the ordered mesostructures. When the molecular weight is higher than 5000, macrophase separation occurs easily during the EISA process, because of the resol's insolubility in ethanol under neutral conditions. Another advantage for choosing resol as a precursor is that it is difficult to evaporate during the EISA process, which results in a constant resin composition with high yield and simultaneous avoidance of the pollution of volatile formaldehyde.

*b. Surfactant Selection.* Choosing a proper template is another key point for the synthesis. The template should interact strongly with the resol precursors and be easily removed. Amphiphilic surfactants such as triblock copolymers containing PEO segments are examples here. Because they contain many oxygen atoms and have a low glass transition temperature (lower than room temperature), PEO–PPO–PEO copolymers can be easily removed at low temperatures without destroying the resin framework. Long alkyl chain ammonium cationic surfactants such as CTAB and nonionic alkyl PEO oligomeric surfactants such as Brij 76 ( $C_{18}H_{35}EO_{10}OH$ ) can also be used as templates to form hybrid resin polymer–surfactant mesostructures. A large

variety of mesostructures can be obtained. However, the templates have not been successfully removed yet, perhaps because of the hard decomposition of the hydrocarbon chain. It can be concluded that PEO–PPO–PEO copolymers are suitable candidates to fabricate organic mesoporous frameworks via organic–organic self-assembly with the same high quality as mesoporous silica structures.

*c. Evaporation and Assembly.* In the second synthesis step (Figure 20), the beginning homogeneous solution is prepared by dissolving the triblock copolymer and resol precursor in ethanol, which is volatile. Owing to the nonvolatility and stability of resol precursors at room temperature, no obvious effects of the ethanol content, the evaporation rate, and the time on the synthesis were observed. Besides ethanol, other organic solvents such as methanol, acetone, and tetrahydrofuran can be used as a solvent. Although water can be used as a solvent, which avoids the water-removal step during the preparation of the resols, the evaporation of water is too slow. It would not be adopted in the present work. The preferential evaporation of ethanol progressively enriches the concentration of the copolymer and drives the organization of resol–copolymer composites into an ordered liquid-crystalline mesophase. Furthermore, the ordered mesophase is solidified by the cross-linking of resols, which can be easily induced by thermopolymerization.

Owing to the successful syntheses of mesoporous silica films, the EISA method is engaged to prepare ordered mesoporous polymer and carbon materials. The EISA method is a strategy that skillfully avoids the cooperatively assembling process between the precursor and the surfactant template. Therefore, the cross-linking and thermopolymerization processes of the resols separate from the assembly.<sup>68</sup> Compared to the hydrothermal synthesis,<sup>57</sup> the EISA method is easier and can produce the mesoporous resins and carbons in a wider synthetic range, including pH value, surfactant, and phenol/template ratio. In the present work, neutral conditions (pH  $\sim$  7) for self-assembly are employed to decrease the polymerization rate of resols, although the mesostructures can also be obtained in a wide pH value range.

*d. Thermopolymerization.* The thermopolymerization step involves cross-linkage and polymerization of the resol resins, further solidification of the ordered mesophases generated by organic–organic assembly, and finally formation of integral 3-D resin frameworks. This step is rather important for the stability of the mesoporous products, because the covalent bonds constructing the framework are essentially formed during this step. A fast rate of resol polymerization would lead to the deformation of preformed mesostructures and even macroscopic phase separation. On the basis of the consideration of the mesophase behaviors of PEO–PPO–PEO copolymers,<sup>69</sup> a relatively low temperature (100 °C) is adopted for thermopolymerization to deliberately decrease the cross-linking rate of the resols. To ensure complete cross-linkage, a long time (>24 h) thermopolymerization is utilized. The FT-IR and NMR results indicate the formation of cross-linking phenolic resin frameworks during this step.

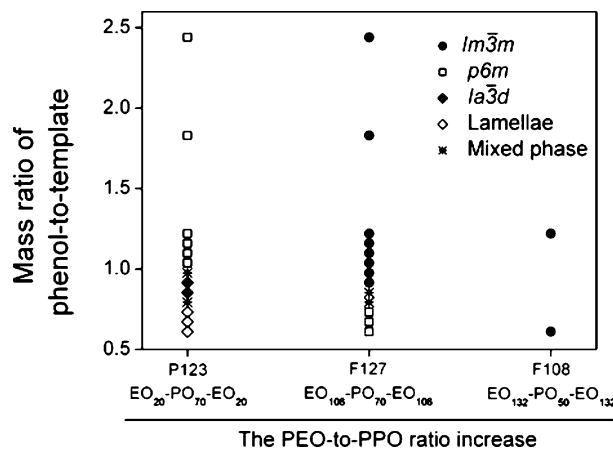


Figure 21. Phase diagram for as-made mesostructured materials.

**2. Control of Mesostructure.** Diverse mesostructures that are lamellar, hexagonal  $p6m$ , cubic  $Ia\bar{3}d$ , and  $Im\bar{3}m$  structures have been synthesized. Figure 21 shows the phase diagram of mesostructures templated by copolymers used in this work. It is found that the final mesostructure depends on the ratio of phenol to template. A sequence of mesostructures, from lamellar to bicontinuous cubic and then to hexagonal, is derived with increasing phenol/P123 ratio. It is known that the phase transformation of liquid crystalline mesophases is from lamellar to bicontinuous cubic, hexagonal, and body-centered cubic as the hydrophilic–hydrophobic balance number grows. As a result of the strong interactions via H-bonds between the resol precursor and the hydrophilic blocks, the precursor favors incorporation with PEO blocks of the copolymer. This leads to swelling of the hydrophilic volume, while the hydrophobic volume per block remains essentially constant. This asymmetry induces a curvature at the PEO/PPO interface, owing to the connectivity of PEO and PPO blocks, the constraint of constant density, and the minimization of chain stretching. A low ratio of phenol/P123 yields a lamellar mesostructure. As the ratio increases, it cannot support the interfacial curvature corresponding to the changes of the hydrophilic/hydrophobic volume ratio. As a result, the mesostructure shifts to cubic bicontinuous  $Ia\bar{3}d$  and hexagonal  $p6m$  structures. However, the body-centered cubic mesostructure is not obtained in the P123-template system, even when the phenol/P123 mass ratio increases to 2.44. An analogous phase transition has been reported in the case of amphiphilic block copolymer and epoxy resin mixtures,<sup>44</sup> as well as for silicate mesostructures. Similar results are obtained in the copolymer F127 self-assembly system. Adding more F127 template into the synthetic solution can bring about the phase transition from hexagonal  $p6m$  to body-centered cubic  $Im\bar{3}m$  mesostructures. Therefore, the progression of mesostructures induced by triblock copolymers can be understood according to the enlargement of hydrophilic/hydrophobic ratios of resol–surfactant mesophases.

It is then natural to find the influence of the hydrophilic to hydrophobic PEO/PPO ratio of copolymer templates on the final mesostructure. P123 with a low PEO/PPO ratio

(68) Wan, Y.; Yang, H. F.; Zhao, D. Y. *Acc. Chem. Res.* **2006**, *39*, 423.

(69) Alexandridis, P.; Zhou, D. L.; Khan, A. *Langmuir* **1996**, *12*, 2690

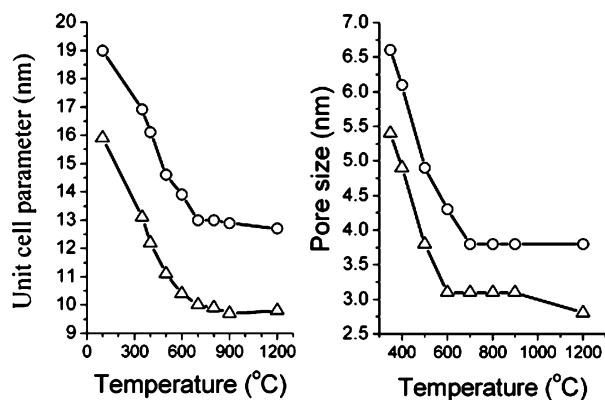


**Figure 22.** Variation of the (a) unit cell parameters  $a$  and (b) pore sizes for calcined FDU-16 (circles) and calcined FDU-15 (triangles) as a function of the calcination temperature.

easily directs the hexagonal FDU-15 structure, similar to that reported for mesoporous silica films. The failure to obtain a cubic  $Im\bar{3}m$  mesostructure, commonly caused by the high hydrophilic/hydrophobic ratio, may also be ascribed to the low PEO/PPO ratio in P123. Perhaps the hydrophilic volume is difficult to swell to a substantial extent. The main product in the F127-template system with a large PEO/PPO ratio is the cubic mesostructure with  $Im\bar{3}m$  symmetry. In this system, the synthetic range for hexagonal FDU-15 mesostructure is quite narrow, and mesostructures of lamellar and bicontinuous  $Ia\bar{3}d$  mesostructures are not yielded in our experimental range. It can be explained that the initial hydrophilic volume is too large to get a low interfacial curvature. Therefore, a higher PEO/PPO ratio in the copolymer may be suitable for the synthesis of body-centered cubic mesostructure. Actually, the only mesostructure is a cubic  $Im\bar{3}m$  mesostructure templated by F108 with a high PEO/PPO ratio. When the phenol/template mass ratio is fixed to 0.61, the mesostructure transforms from lamellar to hexagonal and to body-centered cubic structure with the increase of the template PEO/PPO ratio (Figure 20).

**3. Porosity and Frameworks.** The ability to create accessible mesopores in the mesostructured polymer resins, either by calcination or by extraction, is a consequence of the different thermal stabilities and chemical behaviors of the copolymer templates and the phenolic resins. The PEO-PPO-PEO copolymer template with its high oxygen content exhibits a low thermal stability. In comparison, the stability of phenolic resins is much higher owing to the 3-D network structure constructed by covalent bonds. Mesoporous polymers with large porosity are, therefore, obtained. Further increasing the heating temperature leads to a framework transformation to carbon with ordered homologous mesostructures.

Figure 22 depicts the variation of unit cell parameters and pore sizes of mesoporous materials as a function of heating temperature. These two parameters decrease steadily with temperature and then stabilize above a threshold value of about 600 °C. The sharp declines in the unit cell parameters and pore sizes are due to continuous shrinkage of the frameworks. At least two reasons can be inferred: the removal of templates and the cross-linking reaction of mesostructured resin frameworks. Meanwhile, mesoporous

polymers gradually transform to carbon frameworks by dehydrogenation. Above 600 °C, the shrinkage is slow, suggesting that the carbon frameworks are already formed. As evidence, the weight loss associated with the transformation from phenolic resin to carbon is large, while it is small once the carbon frameworks form. All of our results based on elemental analysis, NMR, FT-IR, XRD, and Raman spectra show that the framework is soft and possesses organic polymer properties when the heating temperature is lower than 600 °C and the framework is rigid and mainly made of amorphous carbons heated above 600 °C. Thereafter, a careful calcination procedure is designed to obtain high-quality mesoporous materials. A low heating rate of 1 °C/min is adopted from room temperature to 600 °C to avoid the collapse of mesostructures due to the large framework shrinkage, while a rapid heating rate of 5 °C/min is programmed above 600 °C.

The porosity can be obtained in FDU-14 and FDU-15 by calcination at 350 °C under Ar but not in caged-like FDU-16 mesostructure. Similar phenomena have been observed with other caged mesostructured materials.<sup>70,71</sup> For example, cubic mesostructured zirconium oxophosphates with caged  $Pm\bar{3}n$  symmetry show high regularity and stability even after heating at 800 °C. However, no porosity can be measured.<sup>70</sup> Similar results are also found in 3-D hexagonal caged mesoporous silica SBA-2 with  $P6_3/mmc$  structure and cubic SBA-16 with  $Im\bar{3}m$  symmetry synthesized at room temperature with the additive of NaOH or Na<sub>2</sub>SO<sub>4</sub>.<sup>3,71</sup> The reason may be that the entrance of the caged pores is too small and occupied by sodium ions or phosphate ions. In our case, the small window of caged-like mesopores of FDU-16 may be blocked by hydrocarbon species which are probably generated by incomplete decomposition of copolymer and concomitant species in polymer resins.

It is, therefore, necessary to add a small amount of oxygen to the heating atmosphere because it can decrease the decomposition temperature and fully remove the template, although the PEO-PPO-PEO copolymer has high oxygen content. However, the organic framework may also burn. Fortunately, the mesoporous phenolic resin frameworks reported here are stable enough to resist this severe condition owing to their high degree of cross-linking. The ordered mesostructures can be retained even after calcination at 1200 °C under a nitrogen flow containing a little oxygen with a sacrifice in product yield. The presence of a little oxygen favors the formation of large porosity in FDU-16. It is clear that the small amount of oxygen can improve the decomposition of triblock copolymer, oxidize some carbons or hydrocarbon on the surface, open the pore window, and give large porosity. This method can be used to generate large pore mesoporous carbons with various structures by controlling the oxygen amount in the atmosphere. A question that remains is the percentage of the copolymer template in FDU-15 mesostructure that can burn off during the calcination at 350 °C under argon. This amount cannot be determined

(70) Shen, S. D.; Tian, B. Z.; Yu, C. Z.; Xie, S. H.; Zhang, Z. D.; Tu, B.; Zhao, D. Y. *Chem. Mater.* **2003**, *15*, 4046.

(71) Huo, Q. S.; Margolese, D. I.; Stucky, G. D. *Chem. Mater.* **1996**, *8*, 1147.



exactly, because it is hard to distinguish the remaining organic species from the organic framework. On the basis of the NMR, IR, TGA, and  $N_2$  adsorption results, at least it can be considered that the templates are completely decomposed and open pore channels are obtained.

Referring to studies on periodic mesoporous silicates, it is found that the solvent extraction method is much milder than calcination and causes less shrinkage of the framework. When the as-made FDU-15 is refluxed in the 48 wt %  $H_2SO_4$  aqueous solution at around 95 °C for 24 h, porosity can be obtained. A large unit cell parameter of 15.7 nm and a pore size of 7.4 nm are acquired, indicating a small contraction. The successful template removal may be attributed to decomposition of the triblock copolymer by sulfuric acid through ether cleavage. In addition, the acid may act as a catalyst to improve the cross-linkage in the phenolic resin. However, the mesoporous polymer resins have much lower surface area (140  $m^2/g$ ) and pore volume (0.26  $cm^3/g$ ) compared with those of calcined FDU-15-350N (Table 1). The NMR results indicate that the copolymer templates in the FDU-15 mesostructure were almost totally decomposed after the reflux. Consequently, the low porosity is attributed to low microporosity and thick pore walls ( $\sim 8.3$  nm). On the basis of an ideal cylinder model, the calculated BET surface area is 118–139  $m^2/g$  when the density of the resin framework is assumed to be 1.1–1.3  $g/cm^3$  according to the previous reports.<sup>72</sup> This implies that the low BET surface area of  $H_2SO_4$ -treated mesoporous polymers is reasonable.

As described above, the amount of residue from the decomposition of templates by sulfuric acid-aided extraction is undetectable. Furthermore, this method is only available to decompose the template in the FDU-15 mesostructure. It may be more favorable to release the low-molecular-weight fragments of the template in hexagonal channels than those in the caged-like structure of FDU-16 and the helix structure of FDU-14.

The BET surface areas and pore volumes increase in the temperature range up to 1200 °C. This can be ascribed to the formation of pores, especially micropores, on the thick pore walls which are generated by the release of low-molecular-weight fragments upon calcination. This result is confirmed by the  $t$ -plot results from  $N_2$  sorption measurements. Estimated by an ideal cylinder model and the carbon-framework density of 1.8–2.1  $g/cm^3$ ,<sup>73</sup> the surface area of mesoporous carbon is calculated to be only 73–66  $m^2/g$ . Therefore, the micropores provide the primary contribution to the surface areas. This can also explain the fact that the surface areas of the mesoporous carbon samples are not as high as for activated carbons. The former have larger uniform mesopore sizes and thicker pore walls, while the latter possess more abundant micropores.

Notably, the heating process has little effect on the mesopore wall thickness, which can be seen in Table 1. The thicknesses of pore walls in FDU-15 materials are calculated to be 6–8 nm based on the data of cell parameters and pore sizes, which is higher than those (<6 nm) of mesoporous

silicates reported previously. This may cause the high thermal stability of the mesostructures even after heating at 1400 °C under an inert atmosphere. To our best knowledge, this is the first example of an open framework with ultrahigh stability ( $> 1400$  °C), which arises from covalently bonded construction, an amorphous carbon component, and thick pore walls. Compared with 2-D mesostructured carbon FDU-15, 3-D cubic FDU-16 carbon mesostructure templated by the same copolymer (F127) and heated at the same temperature has a little higher BET surface area (Table 1) and larger pore size (Figure 22), suggesting a little higher stability of the 3-D network.

## Conclusion

A family of highly ordered mesoporous polymer resins and carbons have been synthesized via organic–organic EISA by using commercially available amphiphilic triblock copolymers as templates and low-molecular-weight and water-soluble phenolic resins, resols, as organic precursors. The driving force for the organic–organic assembly is the preferential evaporation of ethanol which induces the organization of the resol–template liquid-crystalline mesophase. A “rigid” cross-linked phenolic resin framework which has abundant hydroxyl groups, analogous to silicate, is able to strongly interact with the amphiphilic triblock copolymer templates. It can be thermopolymerized around the template mesophase by a simple thermal treatment at 100 °C. The resulting 3-D resin frameworks, being more stable than the template, can resist deformation caused by removal of the templates and be directly transformed to ordered mesoporous carbon frameworks. The five-step mechanism for organic–organic assembly has been demonstrated for the first time.

A systematic study has been carried out on the synthesis of the family of highly ordered mesoporous polymer resin and carbon structures. The family members include mesostructures with lamellar, 2-D hexagonal  $p6m$ , 3-D bicontinuous  $1a\bar{3}d$ , and body-centered cubic  $Im\bar{3}m$  symmetries, which are obtained by simply varying the phenol/template ratio and PEO/PPO ratio in the template. The resols may favor interaction with hydrophilic PEO blocks in copolymers, which causes a change of hydrophilic/hydrophobic ratio in the resol–surfactant mesophase and, hence, a difference in the interfacial curvature. Higher ratios favor the formation of mesostructures with higher curvature. For this trend, attractive 3-D cubic FDU-14 with a gyroid bicontinuous mesostructure has been first synthesized by using the EISA method with copolymer P123 as a template. A mesophase diagram is reported for the first time, which facilitates reproduction of the materials by synthetic scientists.

Two methods are exploited to remove the template and get the porosity, and these are calcination under an inert atmosphere and sulfur acid-aided extraction. The calcination atmosphere greatly influences the pore sizes and surface areas of the final mesoporous products. Calcination at 350 °C under Ar can provide the porosity of hexagonal FDU-15 and bicontinuous cubic FDU-14 mesoporous polymers. However, the porosity of 3-D cubic ( $Im\bar{3}m$ ) FDU-16 mesostructure can be obtained at the same temperature when a small amount of oxygen is fed into the inert gas. The presence of oxygen

(72) Ko, T. H.; Kuo, W. S.; Chang, Y. H. *J. Appl. Polym. Sci.* **2001**, *81*, 1084.

(73) Roggenbuck, J.; Tiemann, M. *J. Am. Chem. Soc.* **2005**, *127*, 1096.

facilitates formation of large pore sizes and high surface areas of mesoporous materials. In comparison with thermal treatment, a new method of solvent extraction is a milder method to remove the template, which leads to reduced framework shrinkage and a larger pore size of FDU-15.

Heating the mesoporous polymers causes continuous and distinct framework shrinkage between 350 and 600 °C, due to the cross-linking reaction of phenolic resins. Simultaneously, polymer frameworks transform to carbons. The temperature of 600 °C is critical to distinguish the two kinds of framework constituents. The shrinkage is slow once the carbon frameworks form. Accordingly, the unit cell parameters and pore sizes decrease and then reach a platform. However, the BET surface areas and pore volumes increase in a temperature range up to 1200 °C, mainly caused by the microporosity. Mesoporous carbons with open frameworks exhibit ultrahighly thermal stability up to 1400 °C and mechanical stability up to 500 MPa. Moreover, a reasonably high reverse electronic capacity is shown in mesoporous carbon materials with well-connected pore structure.

**Acknowledgment.** This work was supported by NNSF of China (20233030, 20373013, 20421303, 20407014, and 20521140450), State Key Basic Research Program of PRC (2001CB610506), Shanghai Science and Technology Committee (04JC14087, 03QF14037, 05DZ22313, and 03527001), Shanghai HuaYi Chemical Group, Unilever research institute of China, and Fudan Graduate Innovation Funds. The authors thank Dr. S.H. Xie for experimental assistance. Y.W. thanks China Postdoc Scientific Fund.

**Supporting Information Available:** The characterizations of the products, SAXS patterns of FDU-15-1400 and FDU-16-1400, XRD patterns of FDU-15-1400 and FDU-16-1400, XRD patterns of as-made FDU-16 and calcined FDU-16, SAXS patterns of as-made FDU-16 (F108) and calcined FDU-16 (F108), XRD patterns of FDU-14 and calcined FDU-14, and XRD patterns, FT-IR spectra, wide-angle XRD patterns of as-made FDU-15 and calcined FDU-15, and <sup>13</sup>C NMR spectrum of the resol precursors. This material is available free of charge via the Internet at <http://pubs.acs.org>.

CM060921U